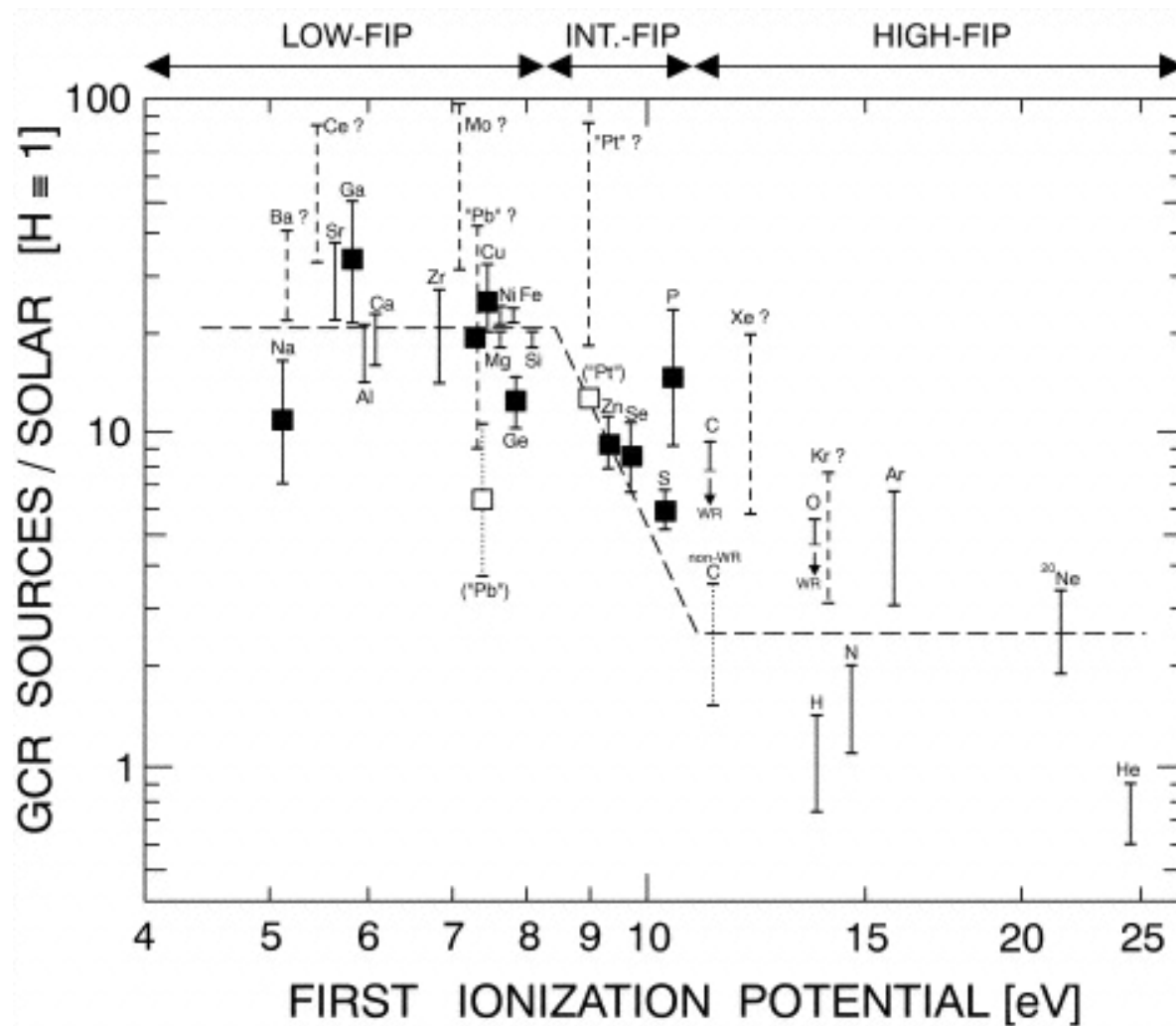
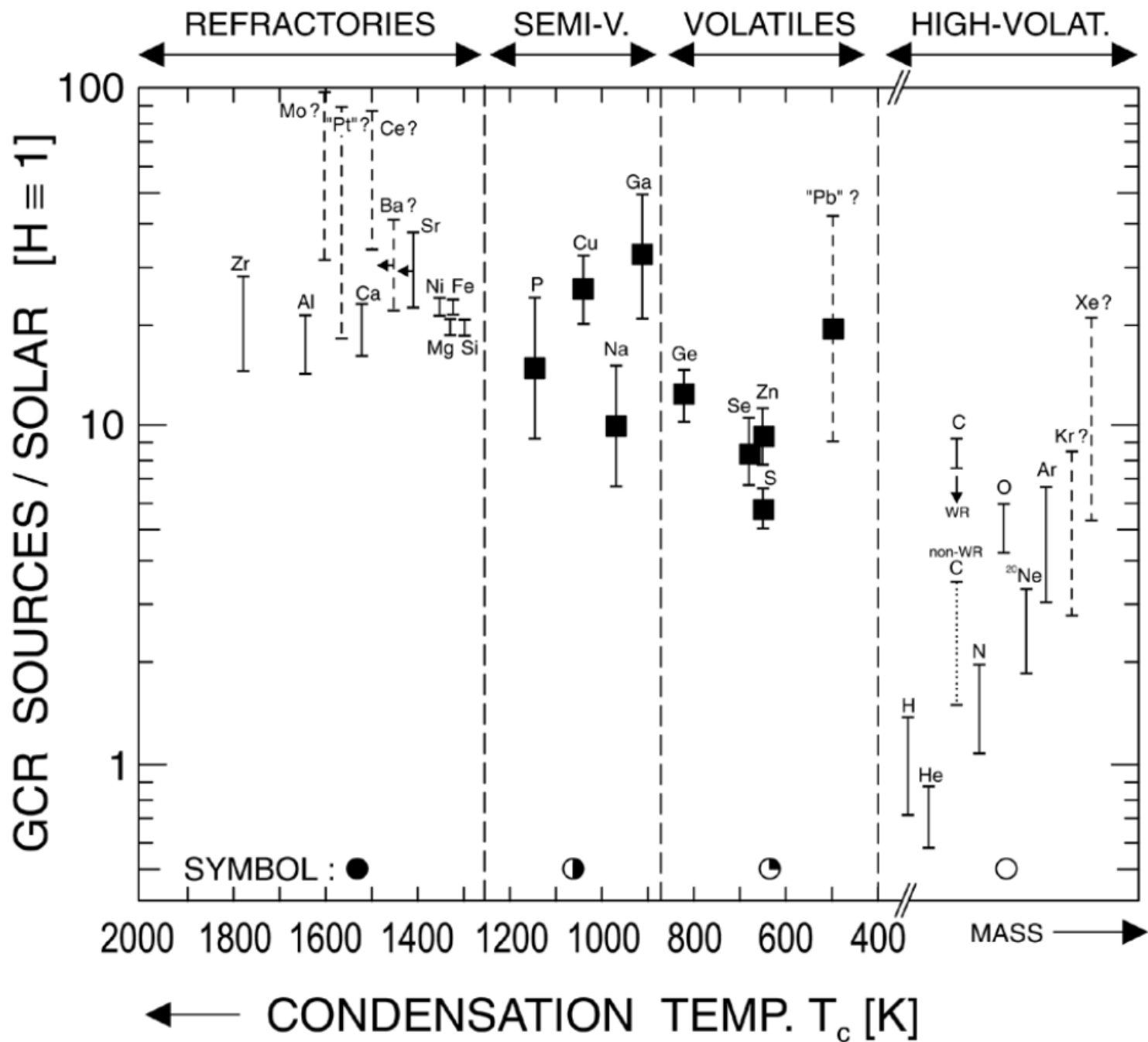


**What are the cosmic-ray
seeds?**

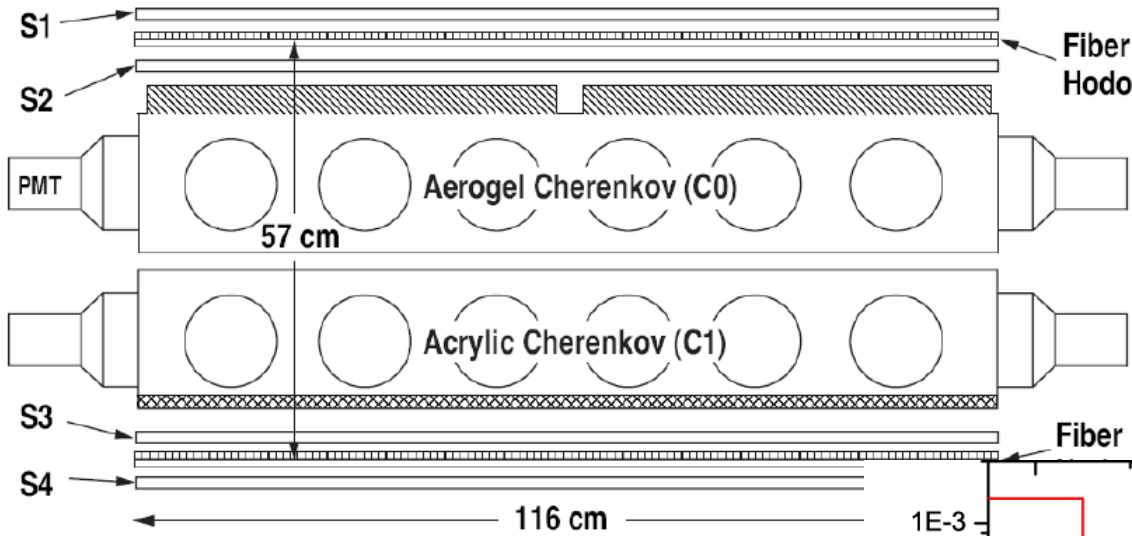
First Ionization Potential





Meyer, Drury
 & Ellison
Ap.J. **487**, 182
 (1997)

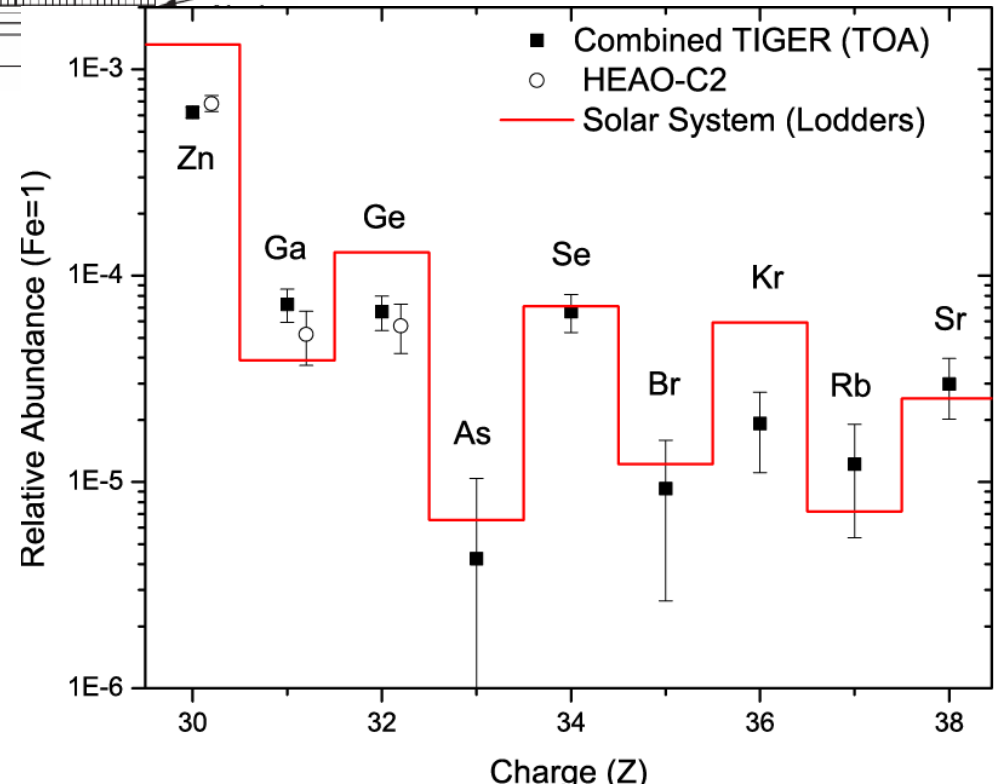
Trans-Iron Galactic Element Recorder



Two balloon flights over Antarctica:

- December 2001 (32 days);
- December 2003 (18 days)

New balloon flight with significantly larger acceptance (Super-TIGER) in December 2012



Rauch et al. *ApJ* **697**, 2083 (2009)

Cherenkov radiation ($\beta > 1/n$)

The light is emitted in a coherent cone (Figure 1.4) at an angle

$$\theta_c = \frac{1}{n\beta}$$

from the direction of the emitting particle. The threshold velocity is thus $\beta = 1/n$, where n is the refractive index of the medium. The presence of a coherent wavefront can be easily derived by using the Huygens-Fresnel principle.

The number of photons produced per unit path length and per unit energy interval of the photons by a particle with charge $z_p e$ is

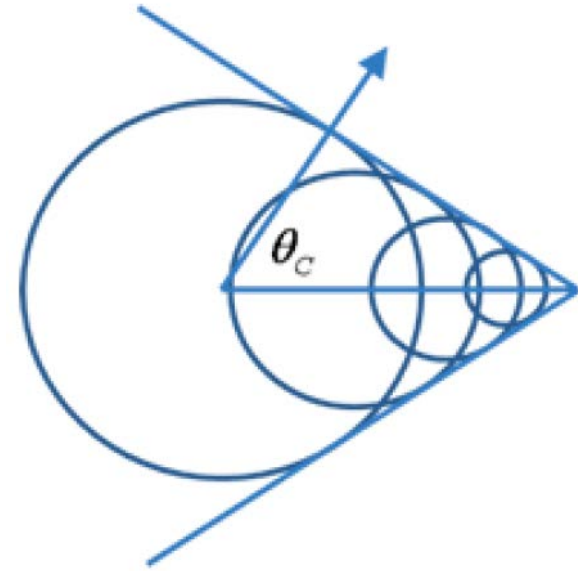
$$\frac{d^2 N}{dE dx} \simeq \frac{\alpha z_p^2}{\hbar c} \sin^2 \theta_c \simeq 370 \sin^2 \theta_c \text{ eV}^{-1} \text{ cm}^{-1} \quad (1.6)$$

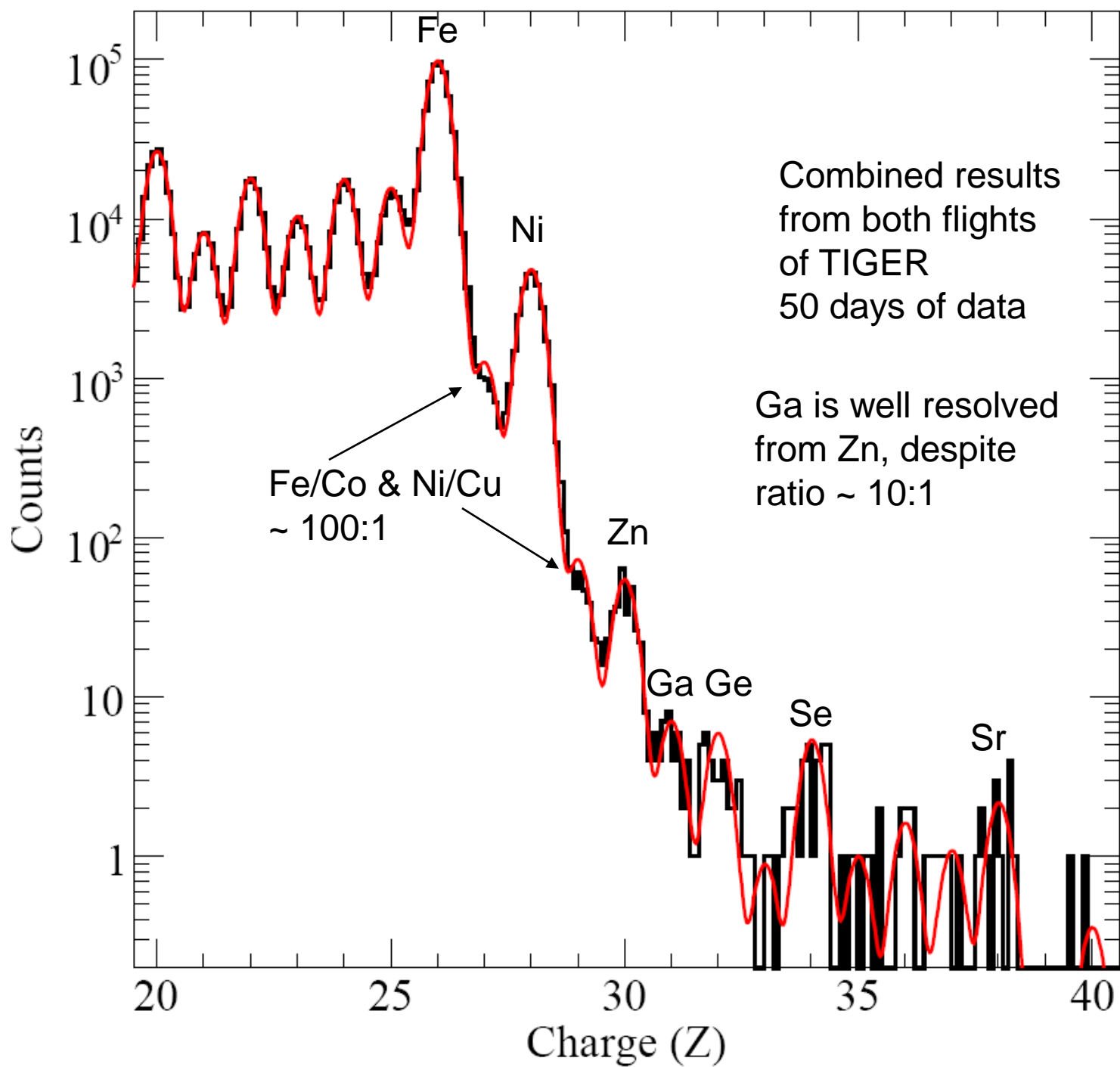
or equivalently

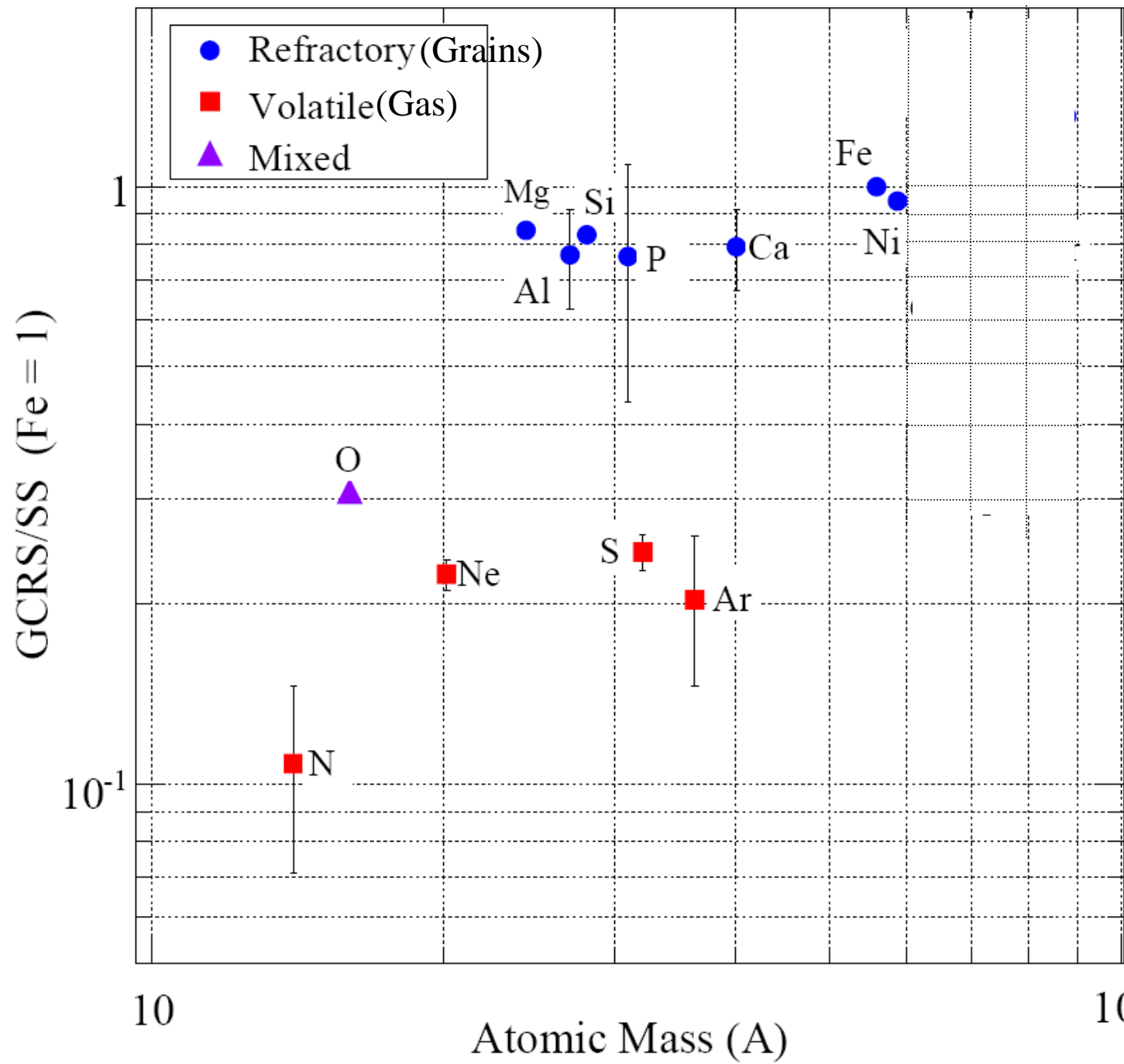
$$\frac{d^2 N}{d\lambda dx} \simeq \frac{2\pi \alpha z_p^2}{\lambda^2} \sin^2 \theta_c \quad (1.7)$$

(the index of refraction n is in general a function of photon energy E ; Cherenkov radiation is relevant when $n < 1$ and the medium is transparent, and this happens close to the range of visible light).

The total energy radiated is small, some 10^{-4} times the energy lost by ionization. In the visible range (300 nm to 700 nm), the total number of emitted photons is about 40 per meter in air, about 500 per centimeter in water. Due to the dependence on λ , it is important that Cherenkov detectors are sensitive close to the ultraviolet region.

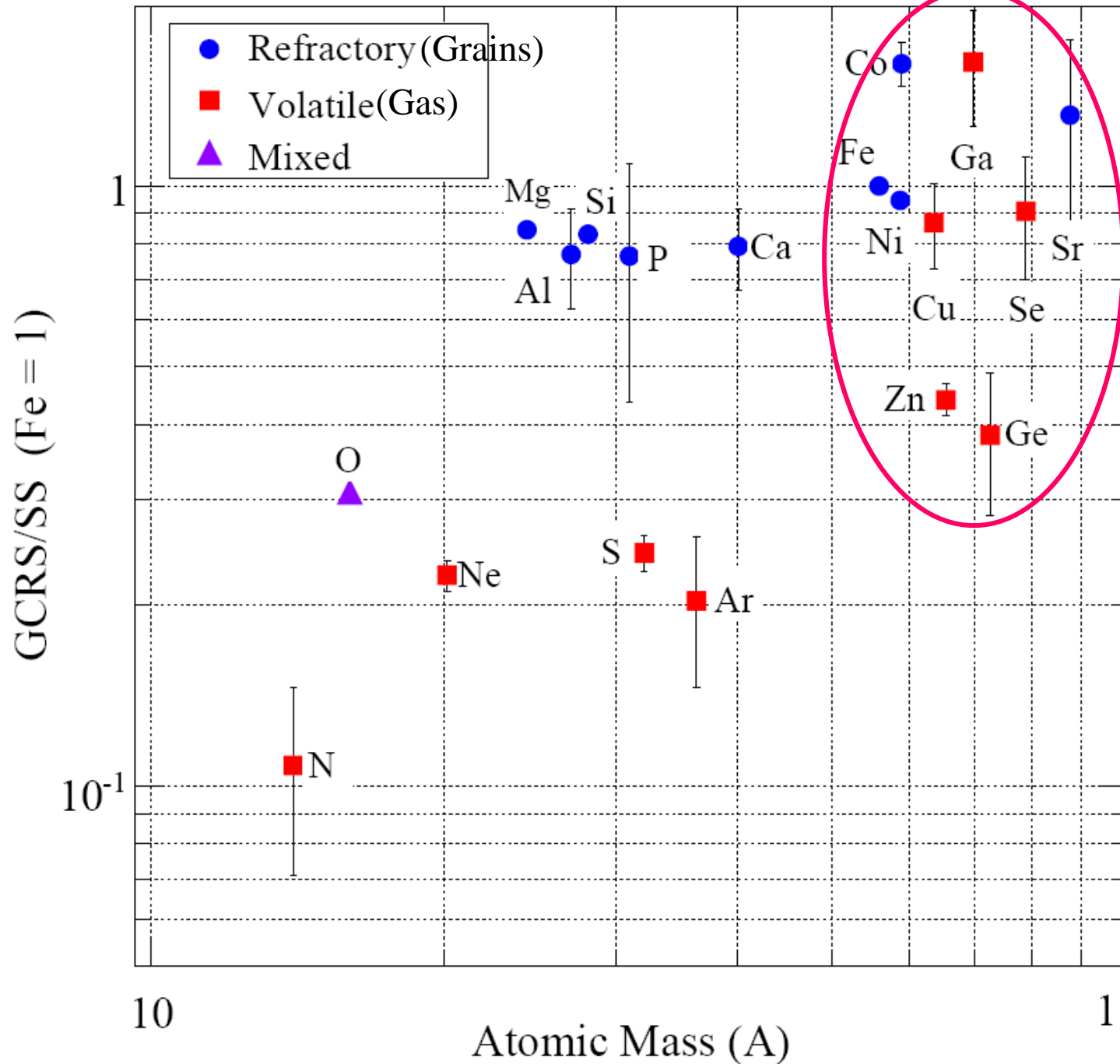






Meyer, Drury, &
Ellison *Ap.J.*
487 182 (1997)

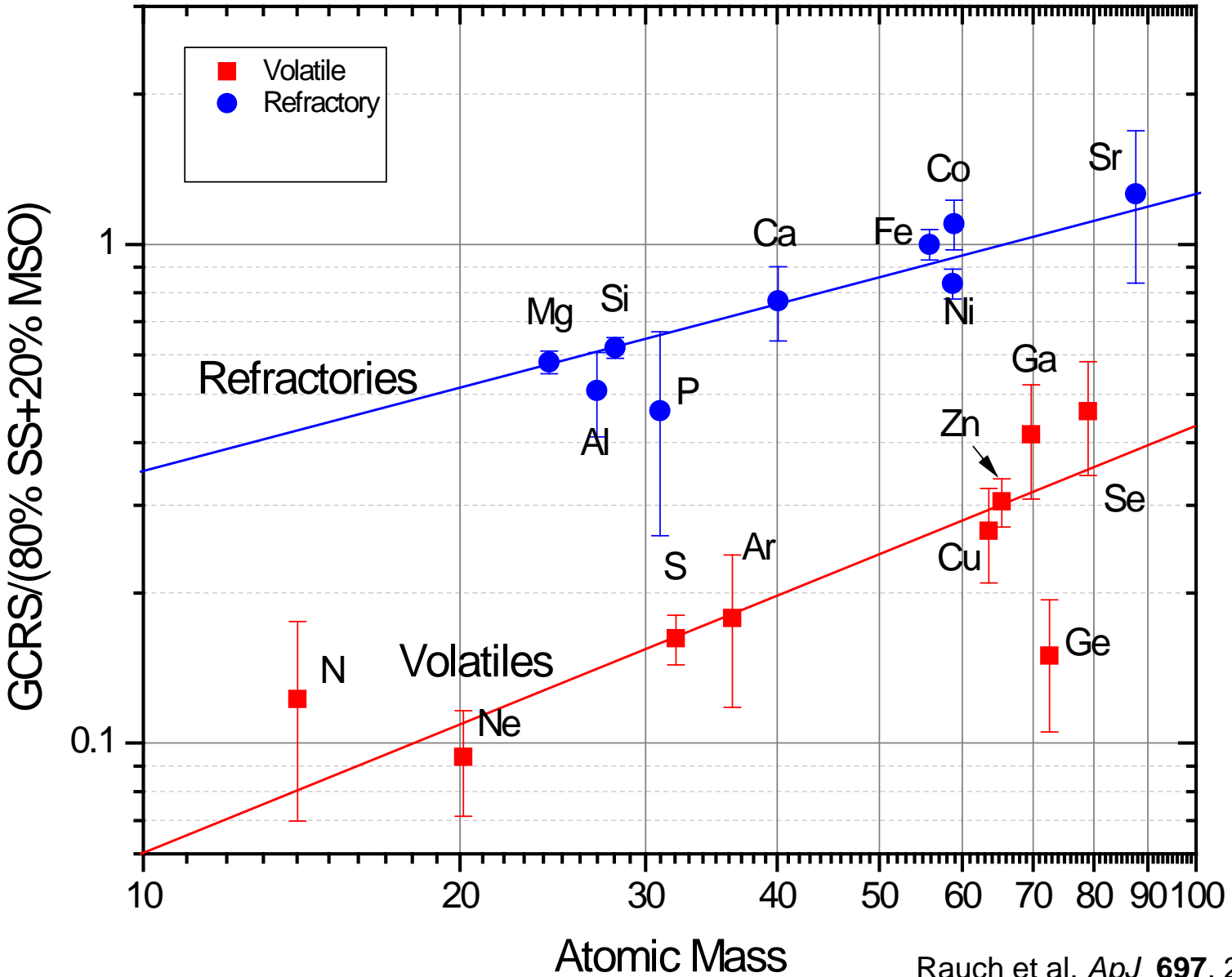
Preferential
acceleration of
elements found
in interstellar
grains, and
mass-dependent
of acceleration
of the volatiles.



There is a lot of scatter here when comparing the cosmic-ray source with solar system.

Meyer, Drury, & Ellison *Ap.J.* **487** 182 (1997)

Preferential acceleration of elements found in interstellar grains, and mass-dependent of acceleration of the volatiles.



Now compare GCR source abundances with a mixture of 80% SS (Lodders) and 20% Massive Star Outflow (Woosley & Heger).

Rauch et al. *ApJ* **697**, 2083 (2009)

Preliminary results of ACE-CRIS for elements $Z > 28$ give results similar to TIGER.

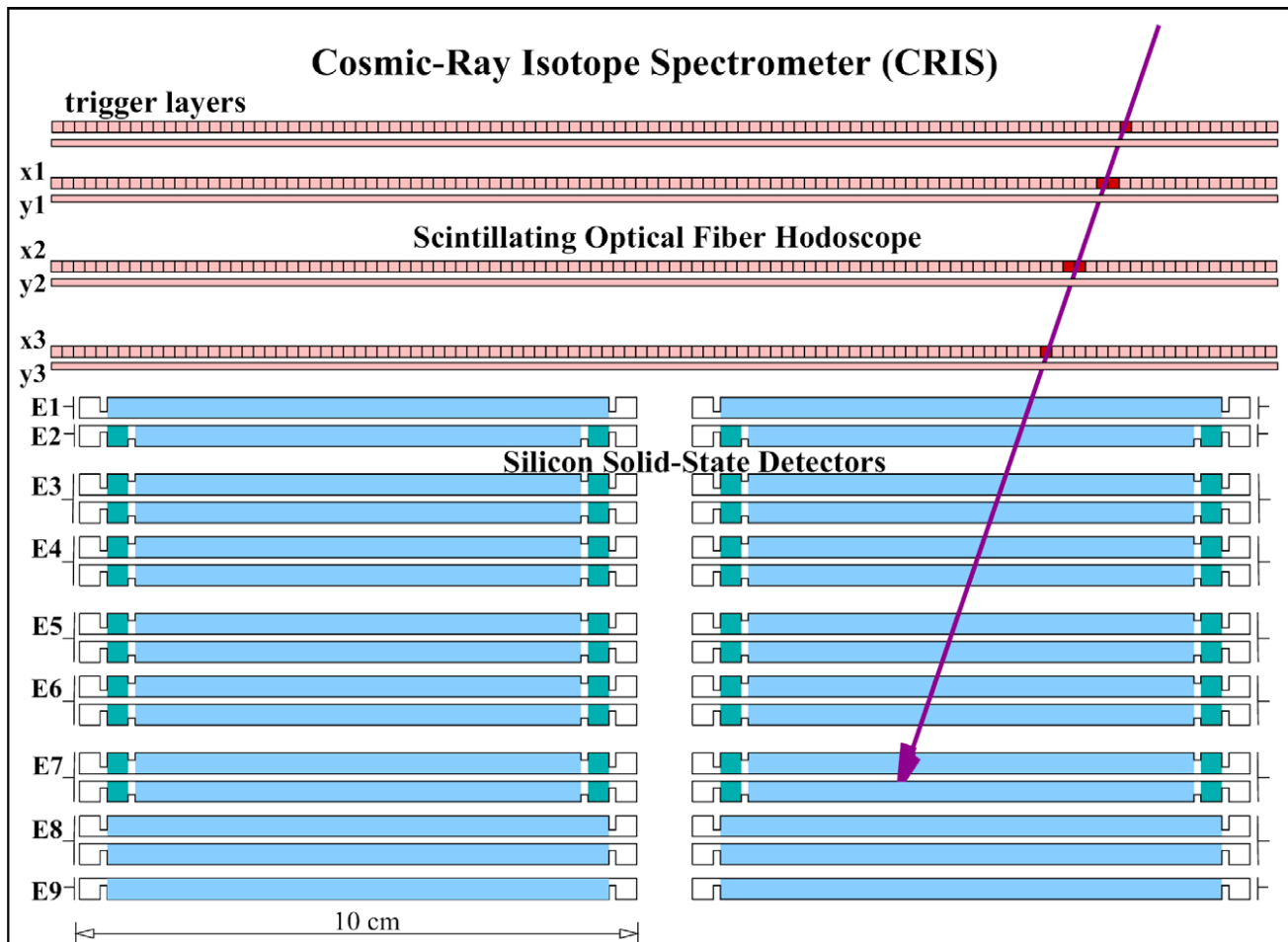
Isotopic Measurements



Cosmic Ray Isotope Spectrometer (CRIS)

Identify isotopes Li-Zn
~50 - 500 MeV/nucleon

Isotopic Measurements



Charged particle interactions

- Charged particles interact basically with atoms, and the interaction is mostly electromagnetic: they might expel electrons (ionization), promote electrons to upper energy levels (excitation), or radiate photons (bremsstrahlung, Cherenkov radiation, transition radiation). High energy particles may also interact directly with the atomic nuclei.

Ionization energy loss

This is one of the most important sources of energy loss by charged particles. The average value of the specific (i.e., calculated per unit length) energy loss due to ionization and excitation whenever a particle goes through a homogeneous material of density ρ are described by the so-called Bethe formula¹. This has an accuracy of a few % in the region $0.1 < \beta\gamma < 1000$ for materials with intermediate atomic number.

$$-\frac{dE}{dx} \simeq \rho D \left(\frac{Z}{A} \right) \frac{(z_p)^2}{\beta^2} \left[\frac{1}{2} \ln \left(\frac{2m_e c^2 \beta^2 \gamma^2}{I} \right) - \beta^2 - \frac{\delta(\beta, \rho)}{2} \right], \quad (4.1)$$

where

- ρ is the material density, in g/cm³;
- Z and A are the atomic and mass number of the material, respectively;
- z_p is the charge of the incoming particle, in units of the electron charge;
- $D \simeq 0.307 \text{ MeV cm}^2/\text{g}$;
- $m_e c^2$ is the energy corresponding to the electron mass;
- I is the mean excitation energy in the material; it can be approximated as $I \simeq 16\text{eV} \times Z^{0.9}$ for $Z > 1$;

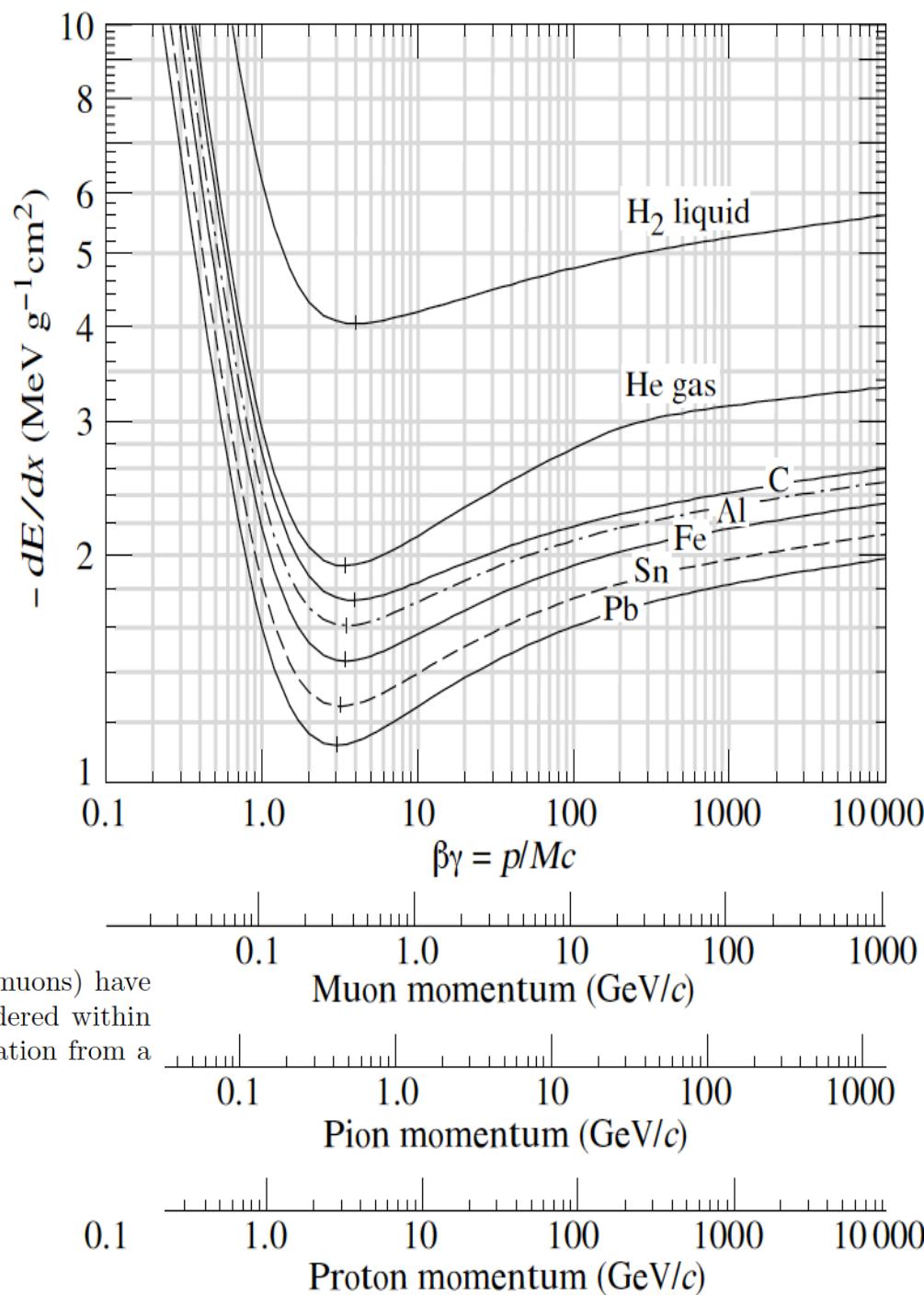
$$-\frac{dE}{dx} \simeq \rho D \left(\frac{Z}{A} \right) \frac{(z_p)^2}{\beta^2} \left[\frac{1}{2} \ln \left(\frac{2m_e c^2 \beta^2 \gamma^2}{I} \right) - \beta^2 - \frac{\delta(\beta, \rho)}{2} \right],$$

The energy loss by ionization (Figure 4.1) is thus in first approximation:

- independent of the mass of the particle;
- typically small for high energy particles (about 2 MeV/cm in water; one can roughly assume a proportionality to the density of the material);
- proportional to $1/\beta^2$ for $\beta\gamma \leq 3$ (the minimum of ionization: minimum ionizing particle, or mip);
- basically constant for $\beta > 0.96$ (logarithmic increase after the minimum);
- proportional to Z/A (Z/A being about equal to 0.5 for all elements but Hydrogen and the heaviest nuclei).

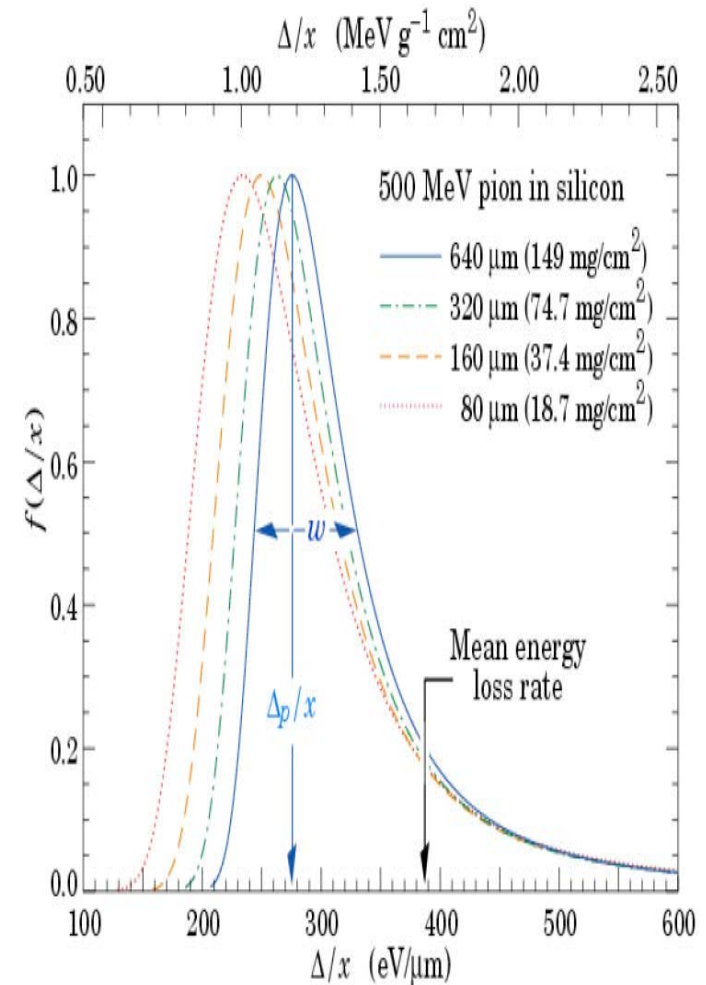
In practical cases, most relativistic particles (e.g., cosmic-ray muons) have mean energy loss rates close to the minimum; they can be considered within less than a factor of two as minimum-ionizing particles. The radiation from a mip is well approximated as

$$\frac{1}{\rho} \frac{dE}{dx} \simeq 3.5 \left(\frac{Z}{A} \right) \text{ MeV cm}^2/\text{g}.$$

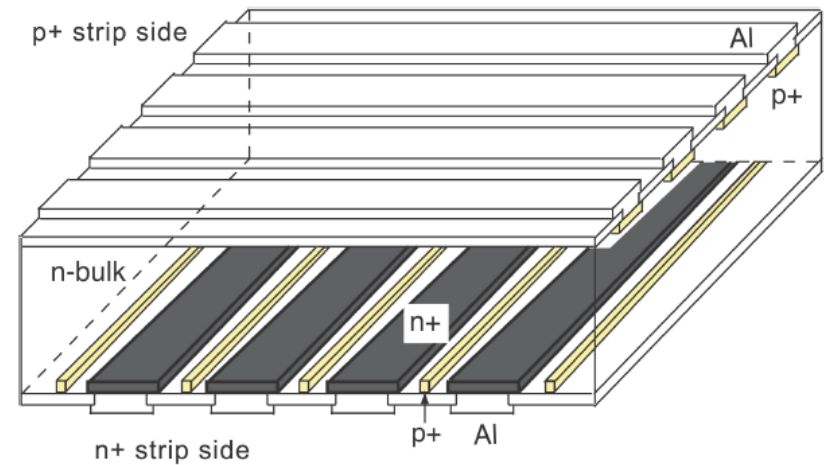


The Landau distribution

The statistical nature of the ionizing process during the passage of a fast charged particle through matter results in large fluctuations of the energy loss in absorbers which are thin compared with the particle range. The energy loss is distributed around the most probable value according to an asymmetric distribution (named the Landau distribution). The average energy loss is about twice as large as the most probable energy loss.



Semiconductor detectors



Silicon microstrip detectors are solid-state particle detectors, whose principle of operation is similar to that of a ionization chamber: the passage of ionizing particles produces in them a number of electron-hole pairs proportional to the energy released.

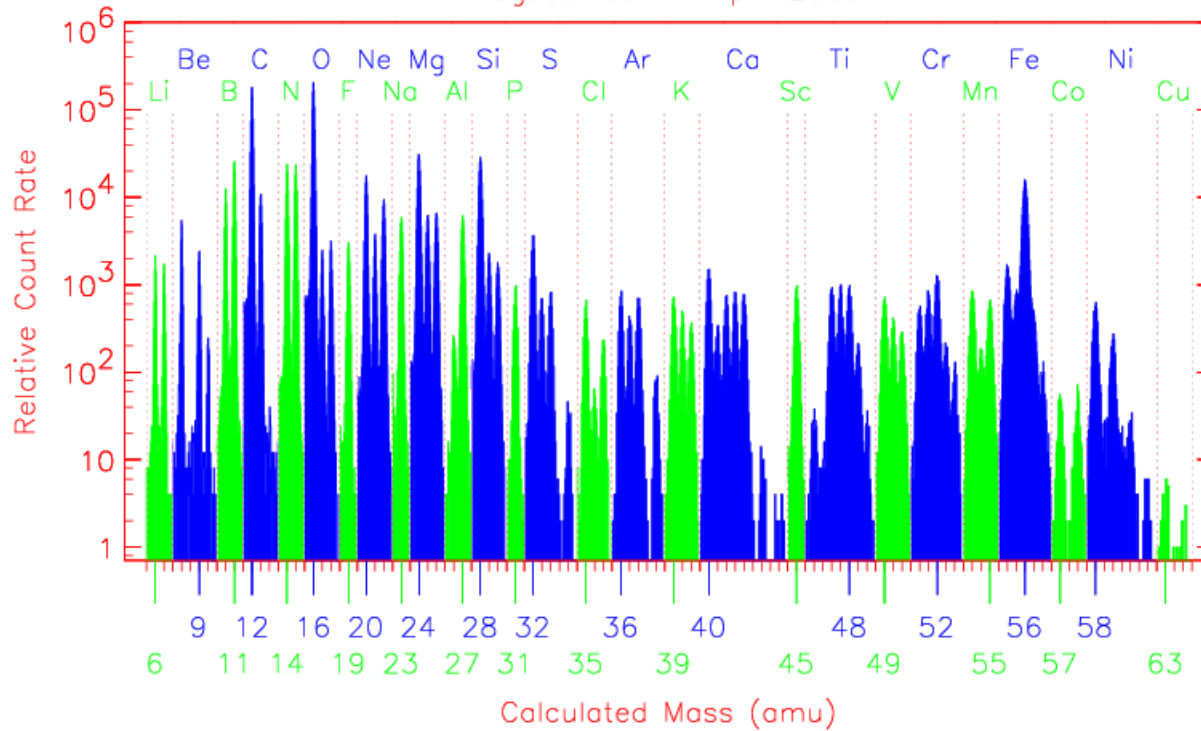
The electron-hole pairs are collected thanks to an electric field, and generate an electrical signal.

The main feature of silicon detectors is the small energy required to create a electron-hole pair – about 3.6 eV, compared with about 30 eV necessary to ionize an atom in an Ar gas ionization chamber.

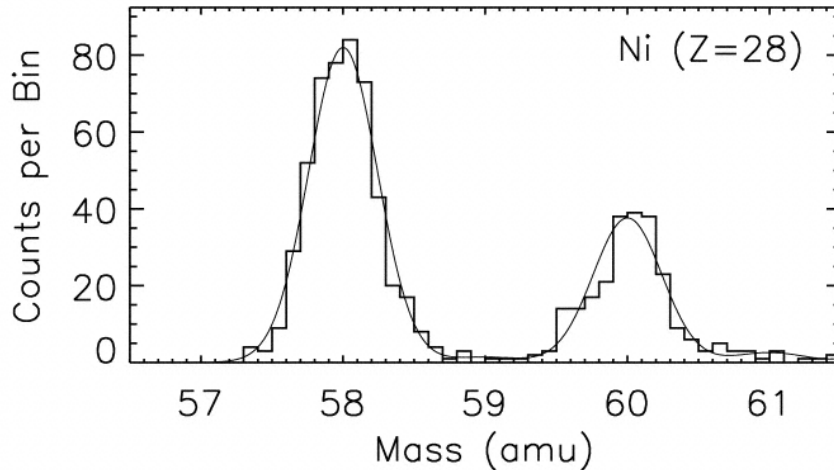
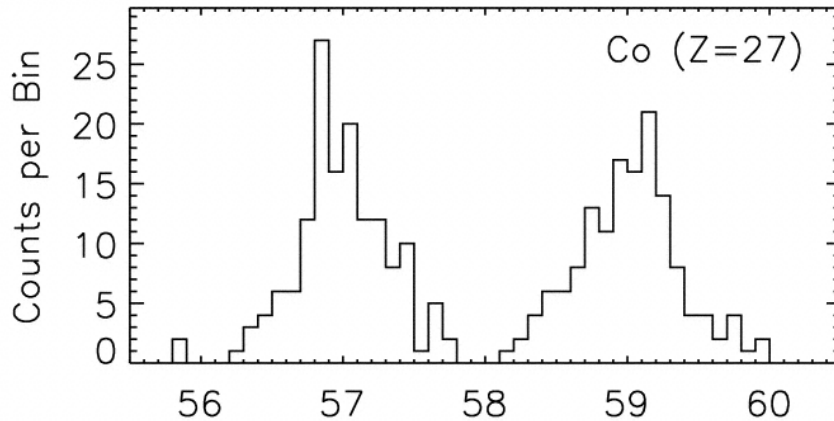
Furthermore, compared to gaseous detectors, they are characterized by a high density and a high stopping power, much greater than that of the gas detectors: they can thus be very thin, typically about 300 μm .

Isotopic Measurements

Cosmic Rays ($\sim 50\text{--}500$ MeV/nucleon)
Measured with the ACE Cosmic Ray Isotope Spectrometer
August 1997 – April 2000



What is accelerated



$^{59}\text{Ni} + e \rightarrow ^{59}\text{Co}$ $T_{1/2} = 0.76 \times 10^5$ years
 β decay is prohibited and the nucleus ^{59}Ni is stable.

During the acceleration phase all electrons are stripped from the atoms. Hence, since ^{59}Ni is absent in the cosmic radiation measured at Earth more than 10^5 years have passed between nucleosynthesis and acceleration. Therefore, it can be inferred that the accelerated material come from the nearby interstellar matter.

However, it is worth noticing, that this is experimentally proved only for the low energy CR component.

Cosmic-ray propagation

CR propagation in the Galaxy

$$\frac{\partial \psi(\vec{r}, p, t)}{\partial t} = q(\vec{r}, p) \text{ sources (SNR, nuclear reactions...)}$$

$$\text{diffusion} + \vec{\nabla} \cdot [D_{xx} \vec{\nabla} \psi - \vec{V} \psi] \text{ convection}$$

$$\text{diffusive reacceleration} + \frac{\partial}{\partial p} \left[p^2 D_{pp} \frac{\partial \psi}{\partial p} \right]$$

$$\text{E-loss} - \frac{\partial}{\partial p} \left[\frac{dp}{dt} \psi - \frac{1}{3} p \vec{\nabla} \cdot \vec{V} \psi \right] \text{ convection}$$

$$\text{fragmentation} - \frac{\psi}{\tau_f} - \frac{\psi}{\tau_d} \text{ radioactive decay}$$

From J. Ormes, ECRS 2004

$\psi(\mathbf{r}, p, t)$ – density per total momentum

Simplified solution: Leaky Box Model

- $\frac{\partial N}{\partial t} = -\frac{N}{\tau_{esc}} + Q(E, t);$

$$Q(E, t) \equiv N_0(E)\delta(t) \rightarrow N(E, t) = N_0(E, t)e^{-\frac{t}{\tau_{esc}}} = N_0 e^{-\frac{x}{\lambda_{esc}}}$$

$\lambda_{esc} = \rho\beta c\tau_{esc}$ mean amount of matter traversed by a particle of velocity βc in the mean time τ_{esc}

- Equilibrium: $\frac{\partial N}{\partial t} = 0$

$$\frac{N_p}{\tau_{esc}} = Q_p - \frac{N_p}{\tau_{int}} \rightarrow N_p = \frac{Q_p(E)\tau_{esc}(R)}{1 + \frac{\lambda_{esc}(R)}{\lambda_p}}, R = \frac{p}{Ze} \text{ GV}/c$$

$$\lambda_{esc} \sim 5 - 10 \frac{g}{\text{cm}^2}, \text{ protons: } \lambda_p \gg \lambda_{esc} \rightarrow N_p \approx Q_p(E)\tau_{esc};$$

$$\tau_{esc} \propto R^{-\delta}, R \cong E \rightarrow N_p \propto E^{-1-\gamma-\delta}, \delta \sim 0.4 - 0.6$$

- Distance travelled: $l = \frac{\lambda_{esc}}{m_p \rho_{ism}}, \rho_{ism} \sim \frac{p}{\text{cm}^3} \rightarrow l \approx 6 \cdot 10^{24} \text{ cm} \approx 2000 \text{ kpc}$

Unstable isotopes of secondary nuclei

- $$\frac{N_s}{N_{pr}} = \frac{\sigma_{pr \rightarrow s}}{\sigma_{pr}} \cdot \frac{\lambda_{esc}}{\lambda_{pr}[1 + \lambda_{esc}/\lambda_s + \tau_{esc}/(\gamma\tau_s)]}$$
- E.g. ^{10}Be unstable to β decay: $\tau_s \approx 2.2 \cdot 10^6 \text{y}$
- If $\tau_{esc} < \tau_{^{10}\text{Be}}$ then measured ratio of unstable to stable beryllium should be comparable to production expectation
- If confinement volume is the galactic disk and $\lambda_{esc} \sim 10 \frac{g}{\text{cm}^2} \rightarrow \tau_{esc} \sim 6 \cdot 10^6 \text{y}$

β -decay secondaries

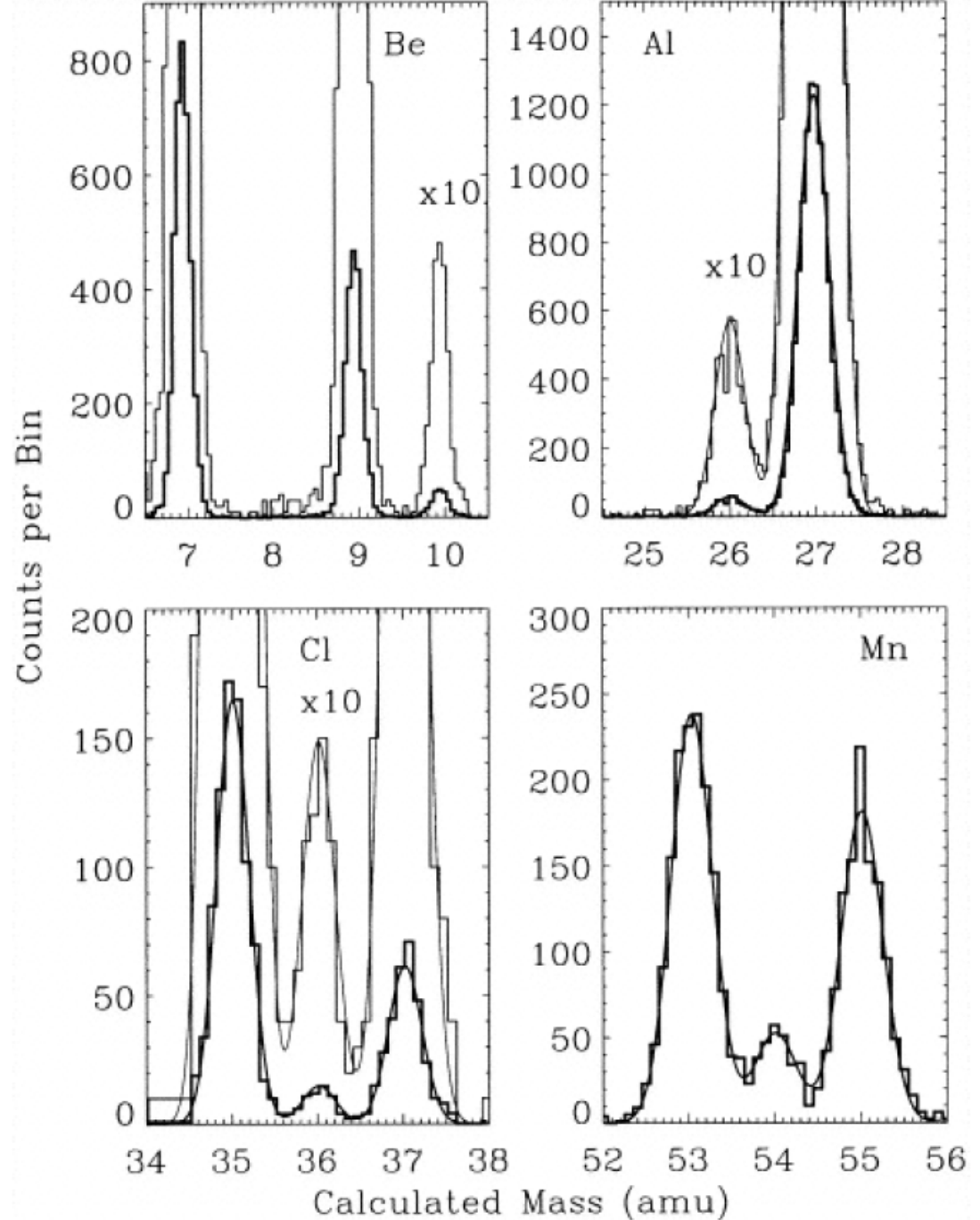
^{10}Be 1.5 Myr

^{26}Al 0.71 Myr

^{36}Cl 0.30 Myr

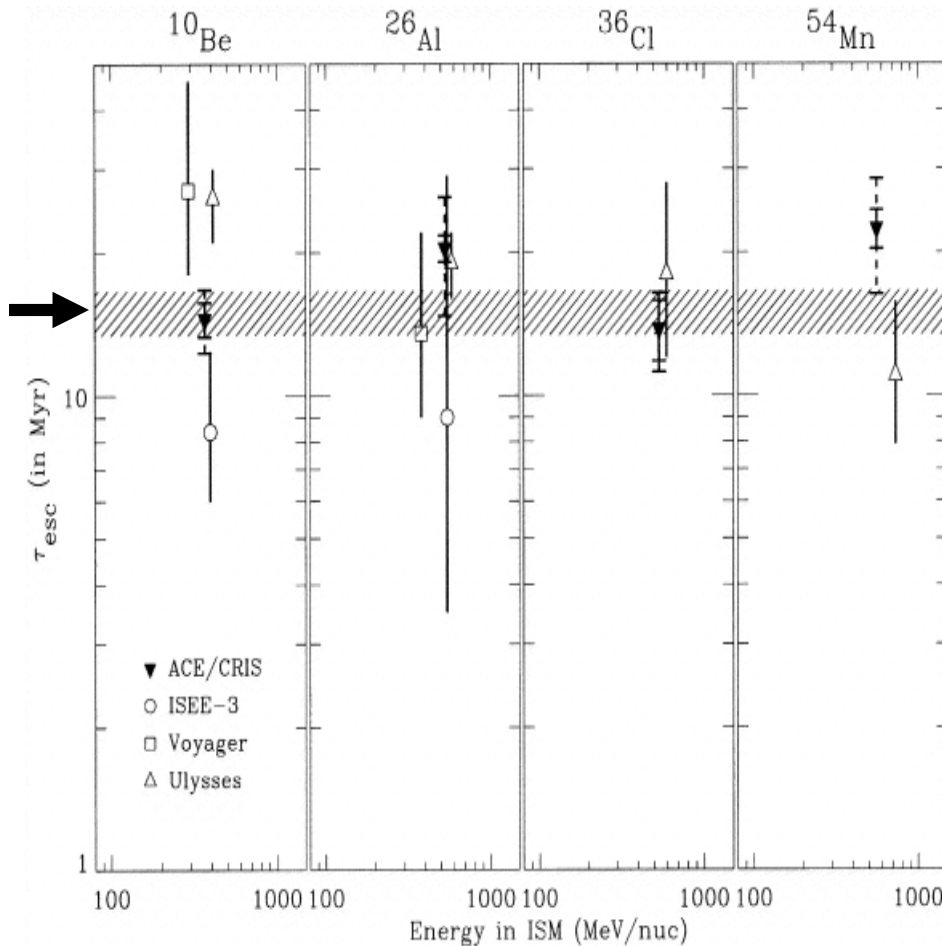
^{54}Mn \sim 0.68 Myr

(Theoretical estimate
of β -decay half life. In
the lab ^{54}Mn decays
by electron capture.)



Confinement time in the Galaxy

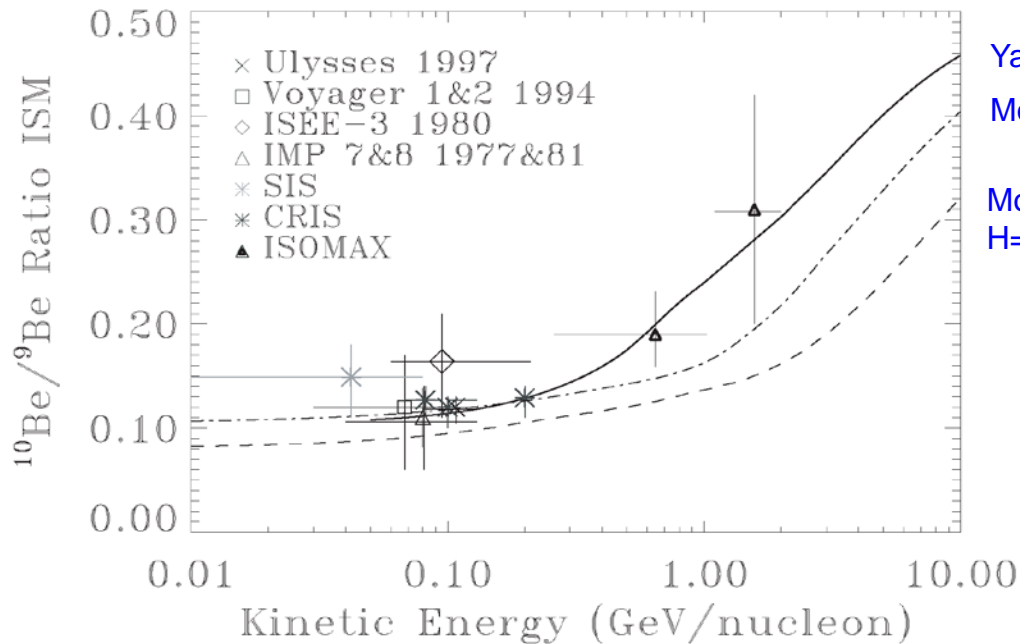
15.0±1.6
Myr



β -decay secondaries
10_{Be} 1.5 Myr
26_{Al} 0.71 Myr
36_{Cl} 0.30 Myr
54_{Mn} ~0.68 Myr
(theoretical estimation of
 β decays, in the lab it
decays for electron)

Yanasak et al., ApJ, **563**
(2001) 768

Propagation in the Galaxy



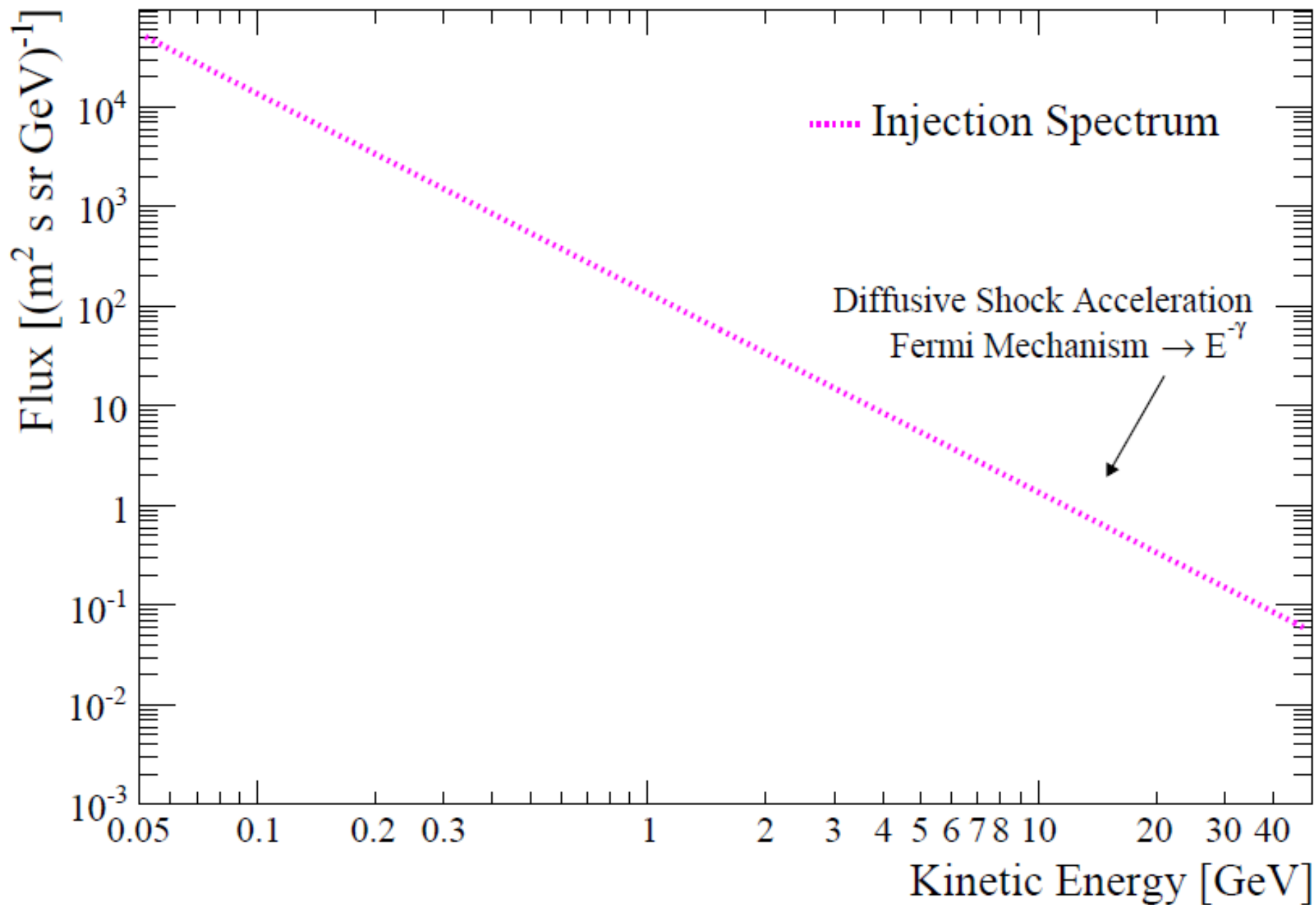
Yanasak et al., ApJ 563 (2001) 768, $n=0.34 \text{ cm}^{-3}$

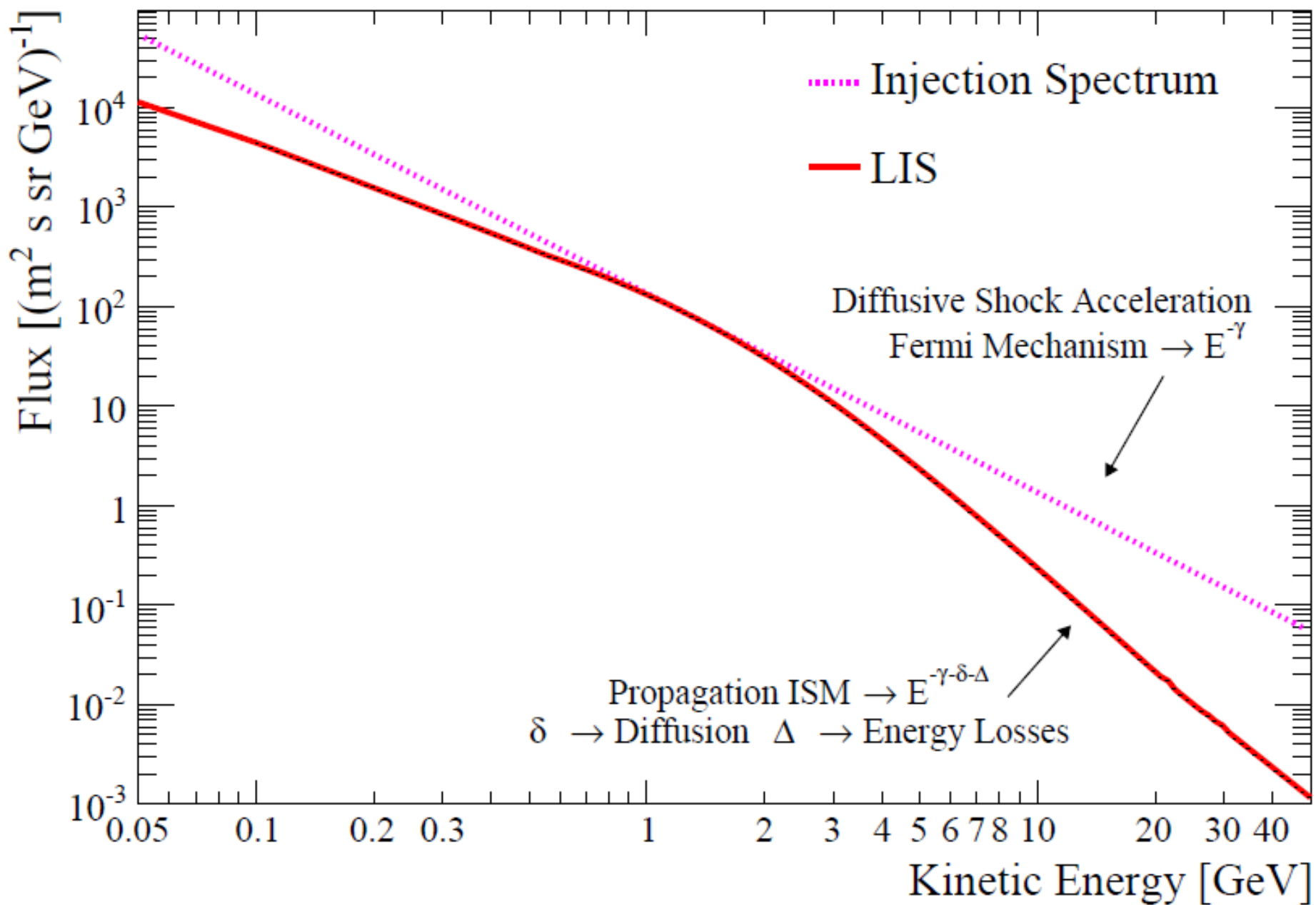
Molnar & Simon, 27th ICRC 1860, $n=0.23 \text{ cm}^{-3}$

Moskalenko & Strong, Ap&SS 272 (2000), 247,
 $H=4 \text{ kpc}$

Hams et al., 27th ICRC, 1655

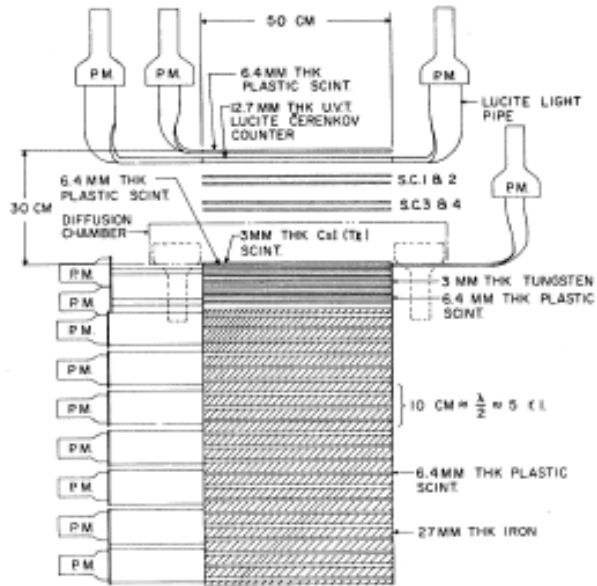
Together with the B to C ratio, the isotopic component ^{10}Be ($^{10}\text{Be}/^9\text{Be}$) can be used to determine parameters of CR propagation models in the Galaxy.





**Cosmic ray energy spectra
(direct detection, $E < \sim 10^{15}$ eV)**

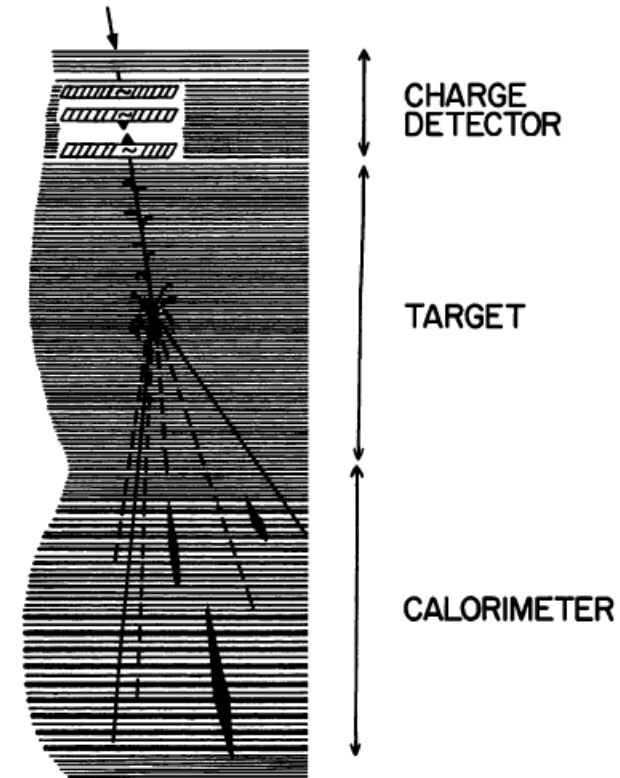
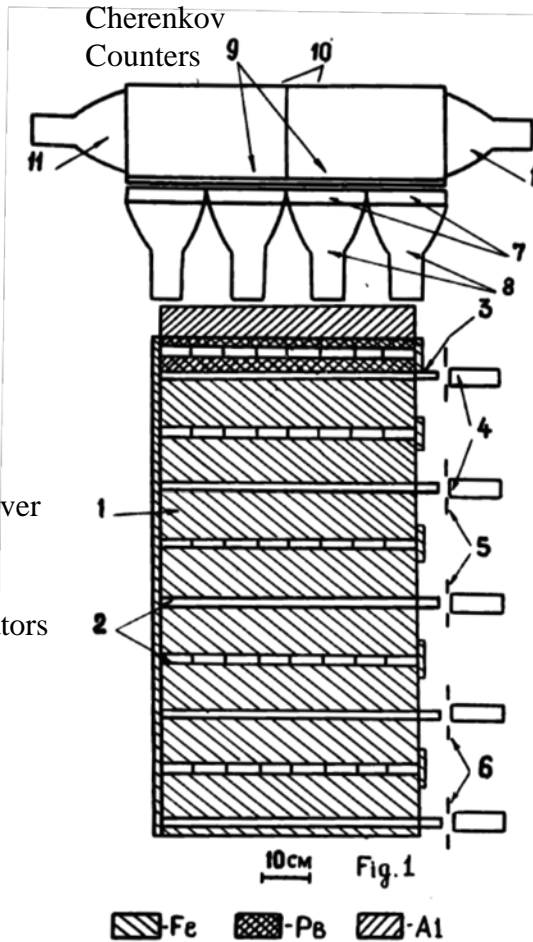
Direct Proton (and Nuclei) Measurements: Calorimeters



Ionization calorimeter absorber

Scintillators

“Ionization Spectrometer” ≡
Calorimeter
(Ryan et al. 1972)

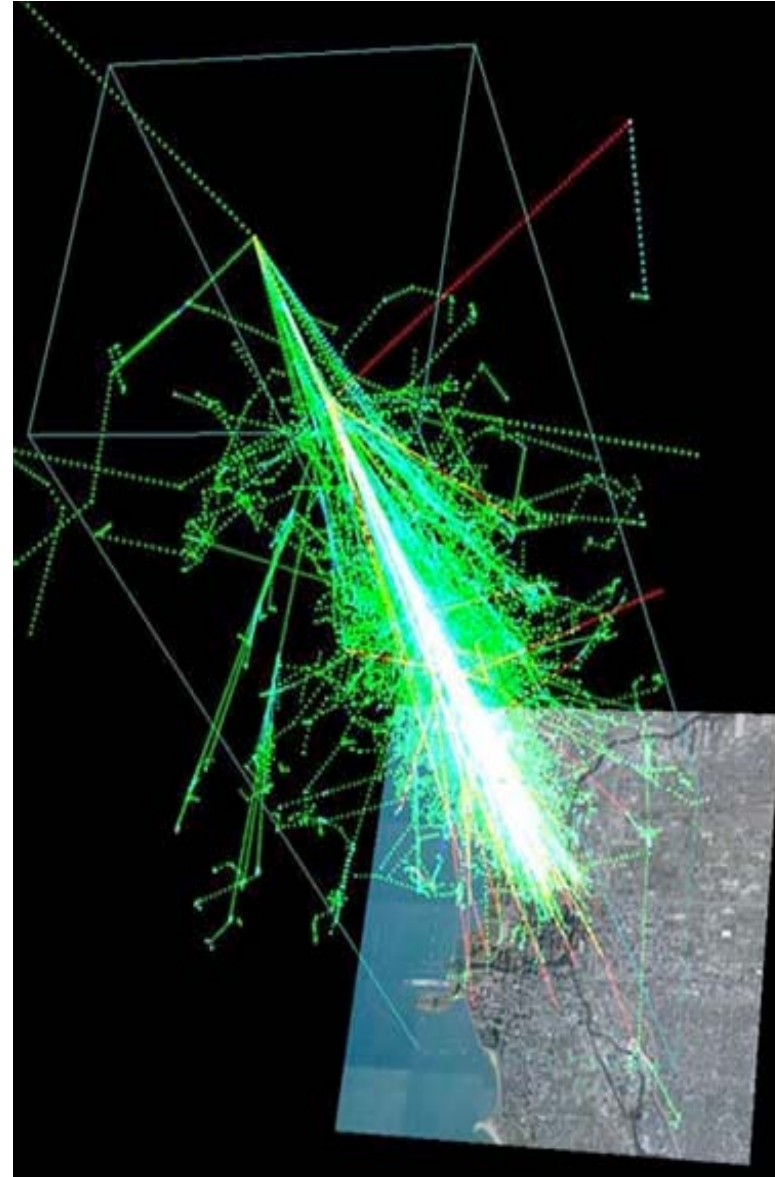


JACEE
(Asakimori et al. 1998)

SOKOL space experiment
(Ivanenko et al. 1993)

Multiplicative showers

- Cascades of particles produced as the result of a primary high-energy particle interacting with matter
 - The incoming particle interacts, producing multiple new particles with lesser energy; each of these interacts in turn, a process that continues until many particles are produced. These are then stopped in the matter and absorbed
- 2 basic types of showers:
 - electromagnetic showers are produced by a particle that interacts via the electromagnetic force, a photon or electron
 - Hadronic showers are produced by hadrons, and proceed mostly via the strong nuclear force
- Same principle, similar detectors, different characteristics (we'll study **electromagnetic showers** in larger detail)



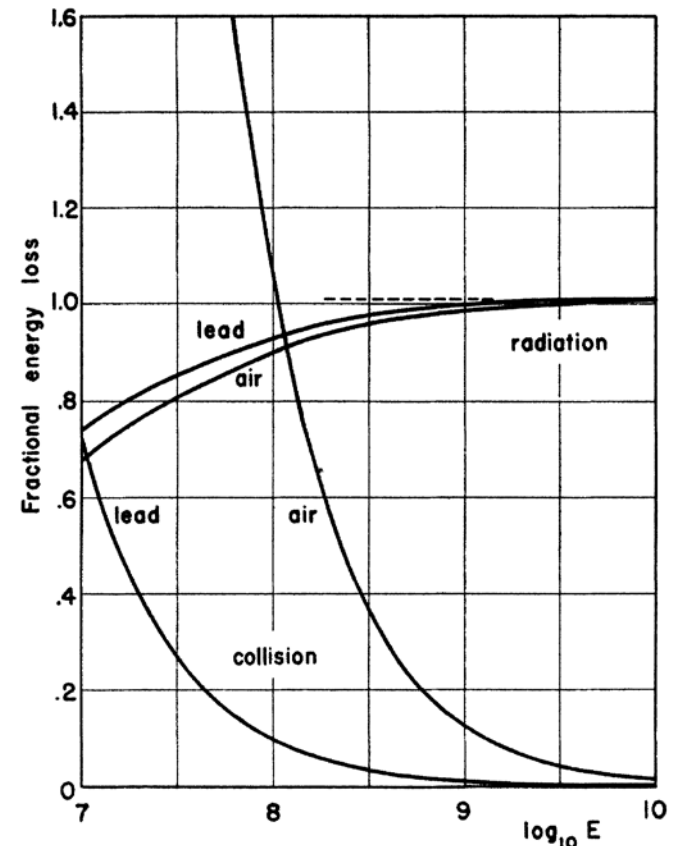
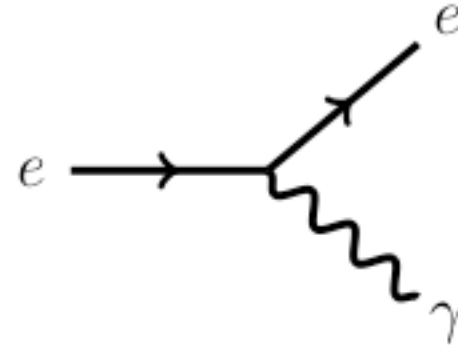
QED HE processes: bremsstrahlung for electrons...

- (and pair production for photons). Forbidden in vacuo by 4-momentum conservation
 - Require interaction with the medium
- **Bremsstrahlung**: photons of momentum $q < E_e$ emitted with probability \sim proportional to $1/q$
 - (and collimated: $\sim m_e/E$)

ie, energy emission is \sim constant for each interval of photon energy; total is propto E

 - The dependence on the material appears through the radiation length X_0 :

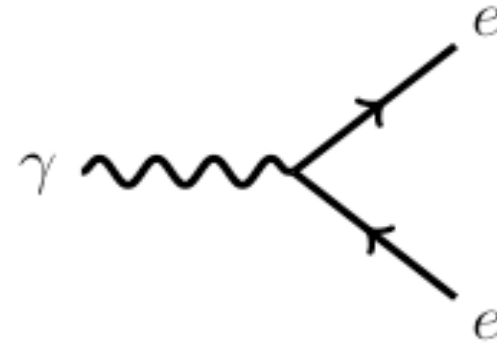
$$dE_e/dx = -1/X_0$$
 - X_0 can be found in tables. It is ~ 400 m for air at NTP, ~ 43 cm for water; for density 1 g/cm^3 roughly proportional to A/Z^2
- Collision energy loss is almost constant (plateau)



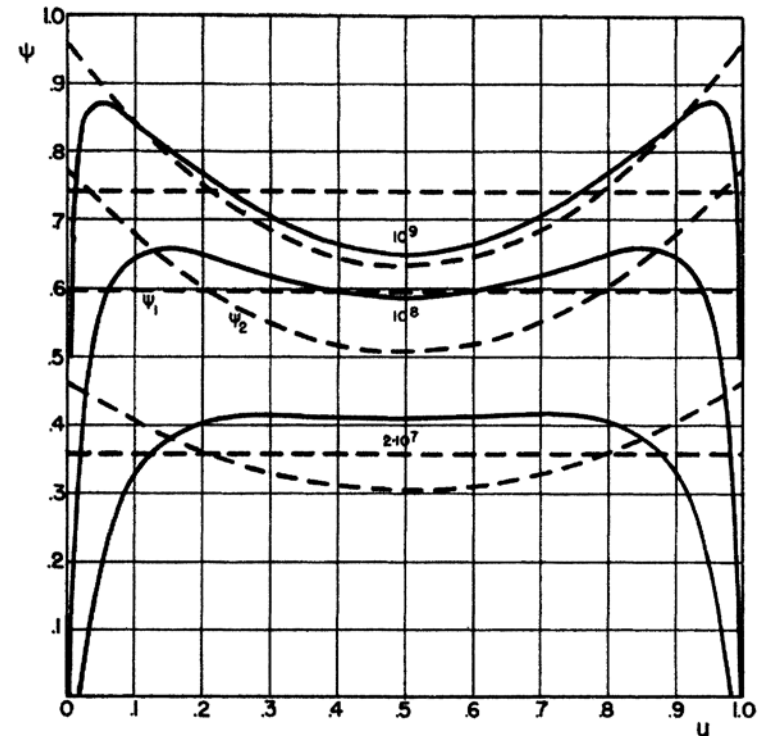
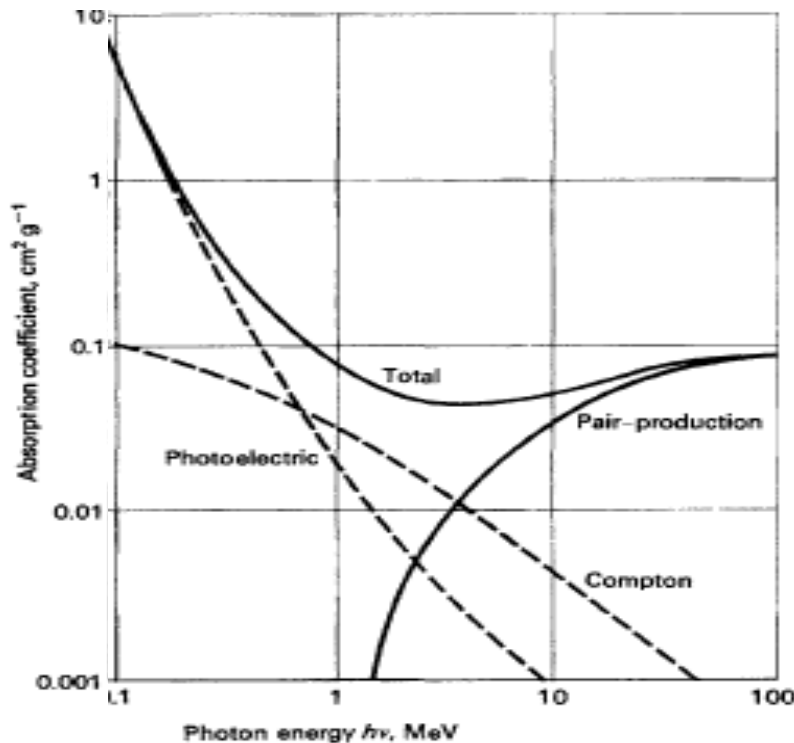
QED HE processes: ...pair production for photons

- Pair production:

$$\lambda = (9/7) \lambda_0 \text{ for } E_\gamma \gg 2m_e$$



Energy spectrum \sim flat



Electromagnetic showers

- When a high-energy e or γ enters an absorber, it initiates an em cascade as pair production and bremsstrahlung generate more e and γ with lower energy
- The ionization loss becomes dominant \ll the critical energy E_c
 - $E_c \sim 84 \text{ MeV}$ in air, $\sim 73 \text{ MeV}$ in water; $\sim (550/Z)\text{MeV}$
 - Approximate scaling in $\gamma = E/E_c$
 - The longitudinal development \sim scales as the radiation length in the material: $t = x/X_0$
 - The transverse development scales approximately with the Moliere radius $R_M \sim (21 \text{ MeV}/E_c) X_0$
 - In average, only 10% of energy outside a cylinder w/ radius R_M
 - In air, $R_M \sim 80 \text{ m}$; in water $R_M \sim 9 \text{ cm}$
- Electrons/positrons lose energy by ionization during the cascade process
- Not a simple sequence: needs Monte Carlo calculations

A simplified approach

- If the initial electron has energy $E_0 \gg E_c$, after t Xo the shower will contain 2^t particles. ~equal numbers of e^+ , e^- , γ , each with an average energy

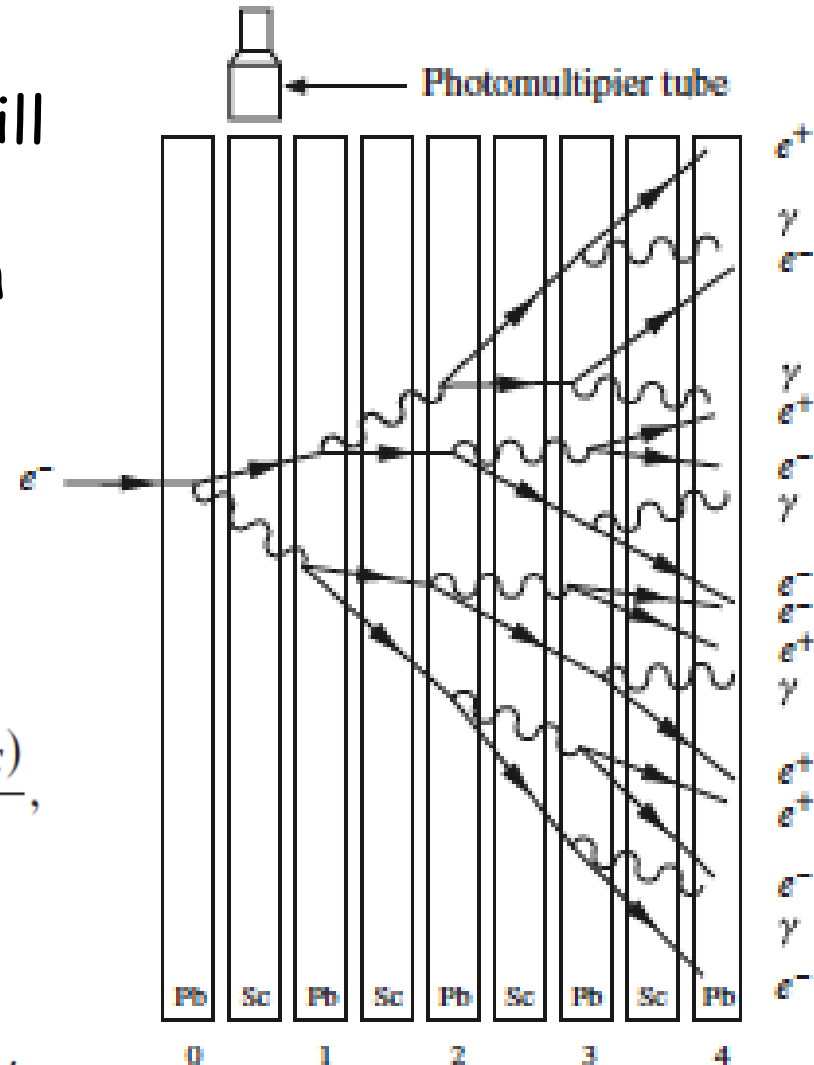
$$E(t) = E_0 / 2^t$$

- The multiplication process will cease when $E(t) = E_c$

$$t_{max} = t(E_c) \equiv \frac{\ln(E_0/E_c)}{\ln 2},$$

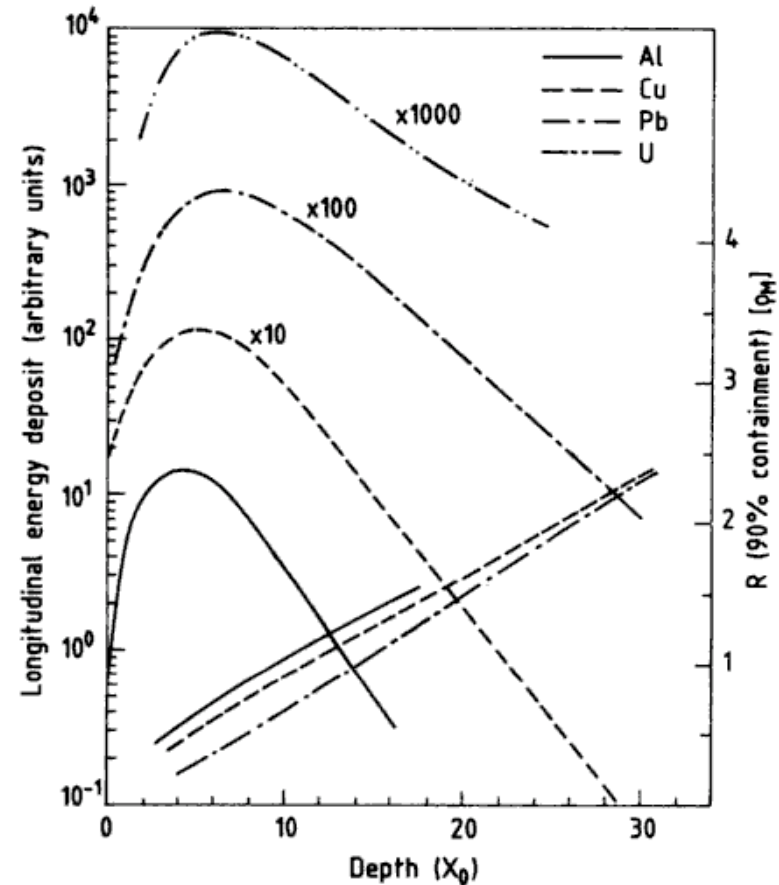
and the number of particles at this point will be

$$N_{max} = \exp(t_{max} \ln 2) = E_0 / E_c$$



An analytic model: Rossi's "approximation B"

- Rossi in 1941 published an analytical formulation for the shower development as a set of 2 integro-differential equations under the approximation that:
 - Electrons lose energy by ionization & bremsstrahlung; asymptotic formulae hold
 - Photons undergo pair production only; asymptotic formulae hold ($E > 2 m_e$)
- Very good approximation until $E \sim E_c$



Incident electron

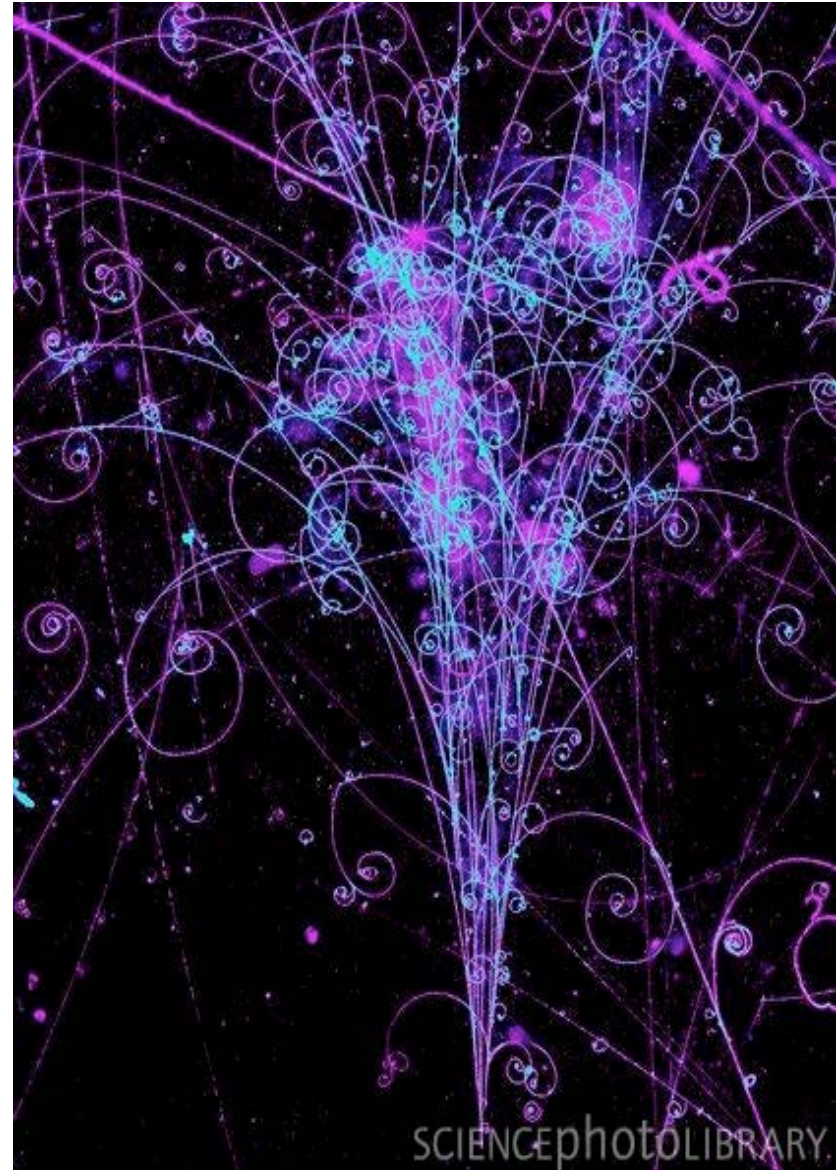
Incident photons

Peak of shower, t_{\max}	$1.0 \times (\ln y - 1)$	$1.0 \times (\ln y - 0.5)$
Centre of gravity, t_{med}	$t_{\max} + 1.4$	$t_{\max} + 1.7$
Number e^+ and e^- at peak	$0.3 y \times (\ln y - 0.37)^{-1/2}$	$0.3 y \times (\ln y - 0.31)^{-1/2}$
Total track length T	y	y

Energy measurement

- The calorimetric approach:
absorb the shower
 - As much as possible... But the logarithmic behavior helps
 - Typically (20-30) X_0 give an almost full containment up to hundreds of GeV
 - But sometimes it is difficult (calorimeters in space)
 - Errors asymptotically dominated by statistical fluctuations:

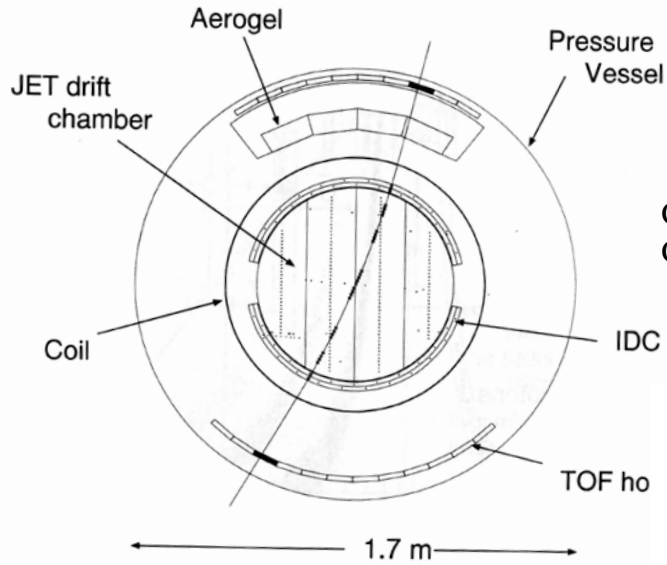
$$\frac{\sigma_E}{E} \cong \frac{k_E}{\sqrt{E}} \oplus c$$



Hadronic showers and calorimeters

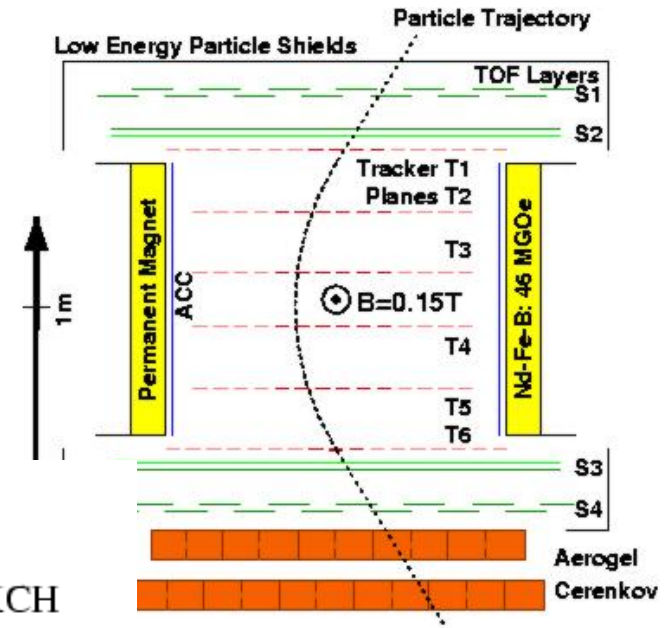
- Although hadronic showers are qualitatively similar to em, shower development is more complex because many different processes contribute
 - Larger fluctuations
 - Some of the contributions to the total absorption may not give rise to an observable signal in the detector
 - Examples: nuclear excitation and leakage of secondary muons and neutrinos
 - Depending on the proportion of π^0 s produced in the early stages of the cascade, the shower may develop predominantly as an electromagnetic one because of the decay $\pi^0 \rightarrow \gamma \gamma$
 - The scale of the shower is determined by the nuclear absorption length λ_H
 - Since typically $\lambda_H > X_0$, hadron calorimeters are thicker than em ones
 - The energy resolution of calorimeters is in general much worse for hadrons than for electrons and photons
 - Energy resolution typically a factor of 5-10 poorer than in em calorimeters
- ⇒ **Go cheap: sandwich**

Direct Proton (and light Nuclei) Measurements: Magnetic Spectrometers



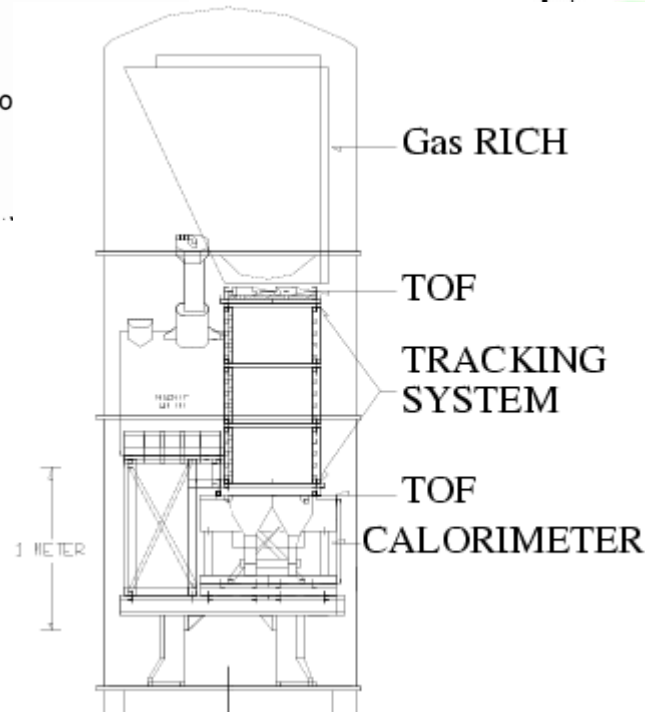
**BESS
(1993-2007)**

Cherenkov
Counters



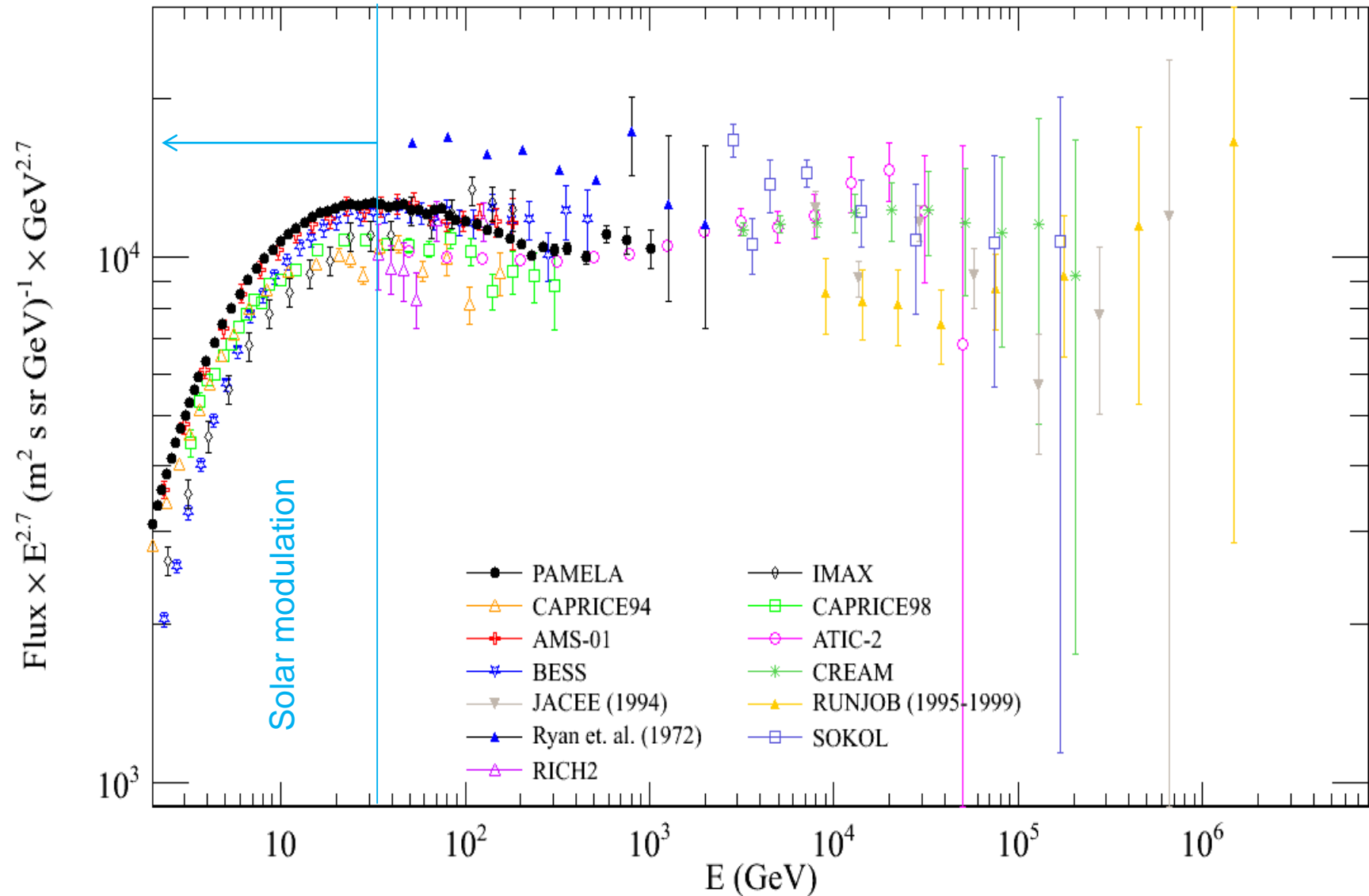
**AMS-01
(Shuttle Flight 1998)**

**Robert Golden's spectrometer:
CAPRICE98 (1998)**



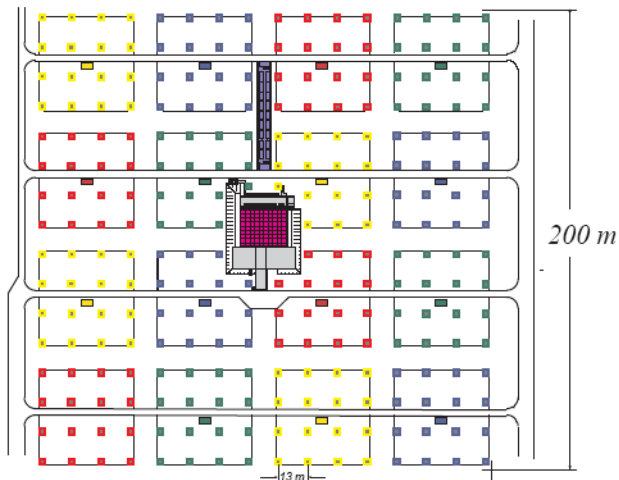
Aerogel
Cherenkov

Proton (Hydrogen) Spectrum



Indirect Proton (and Nuclei) Measurements

experimental setup



KASCADE
(T. Antoni et al.
2003)

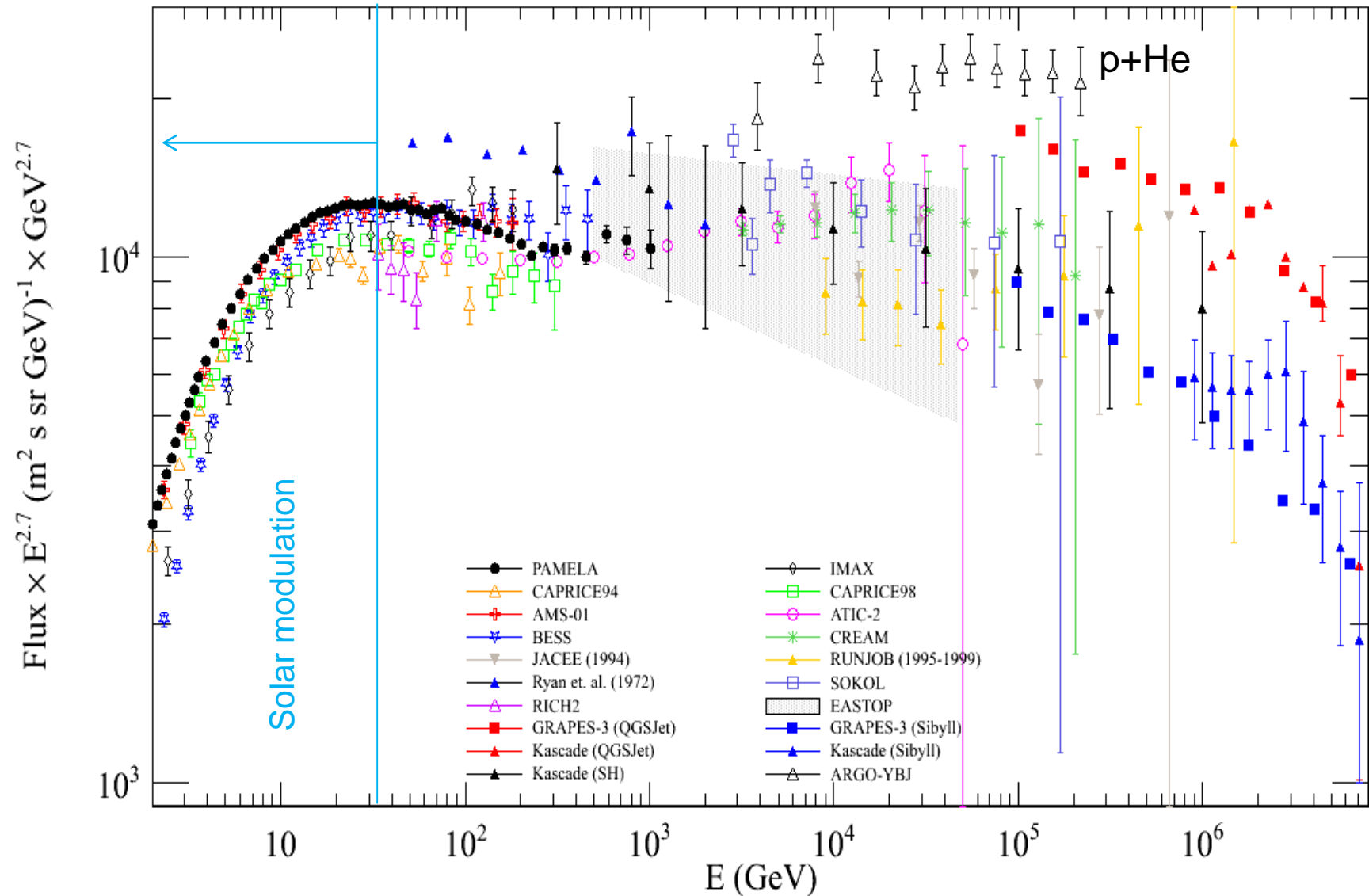


EAS-TOP
(M. Aglietta et al. 2003)

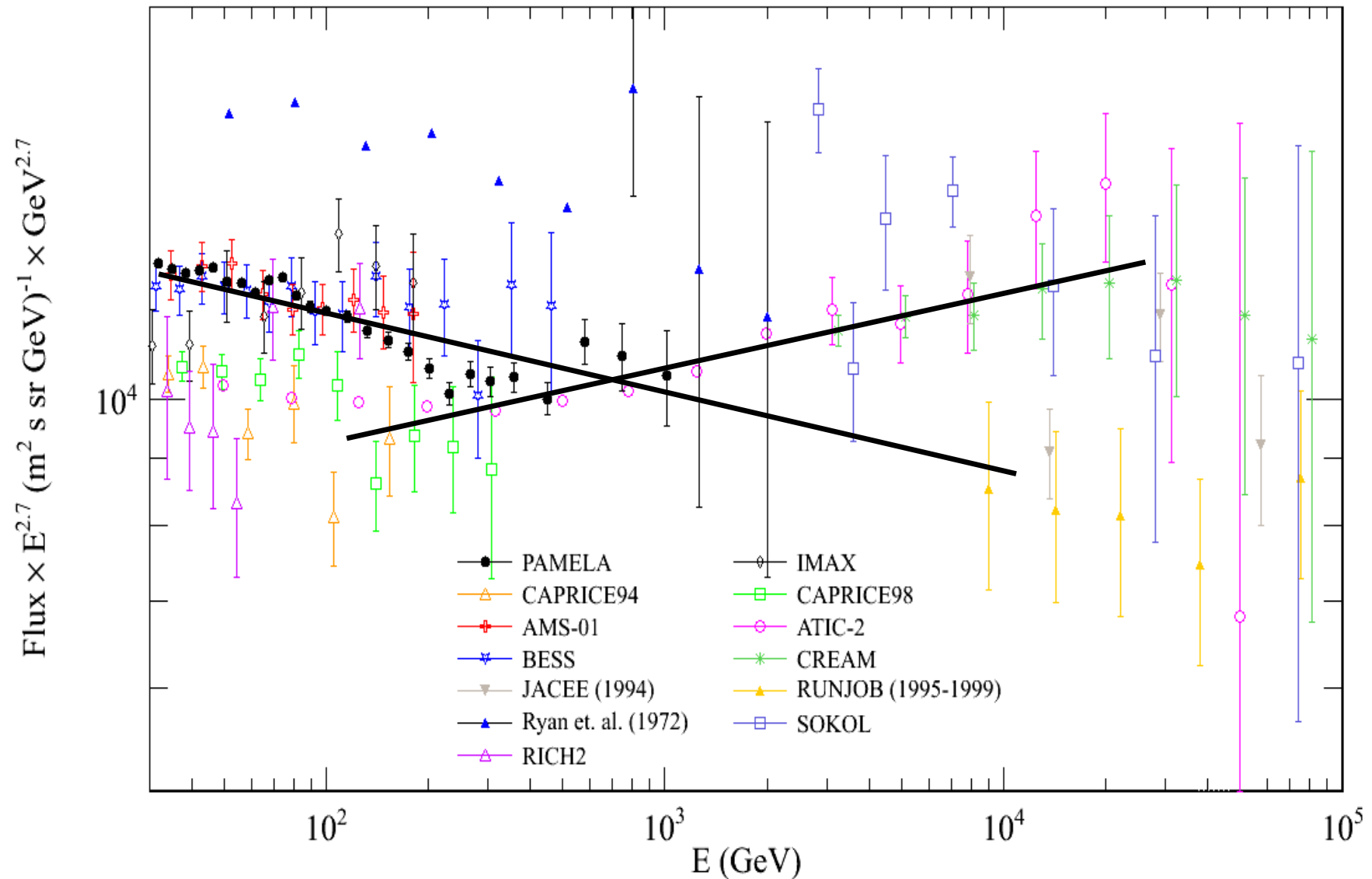
GRAPES
(Y. Hayashi et al. 2005)



Proton (Hydrogen) Spectrum



Proton (Hydrogen) Spectrum



PAMELA detectors

Main requirements → high-sensitivity antiparticle identification and precise momentum measure

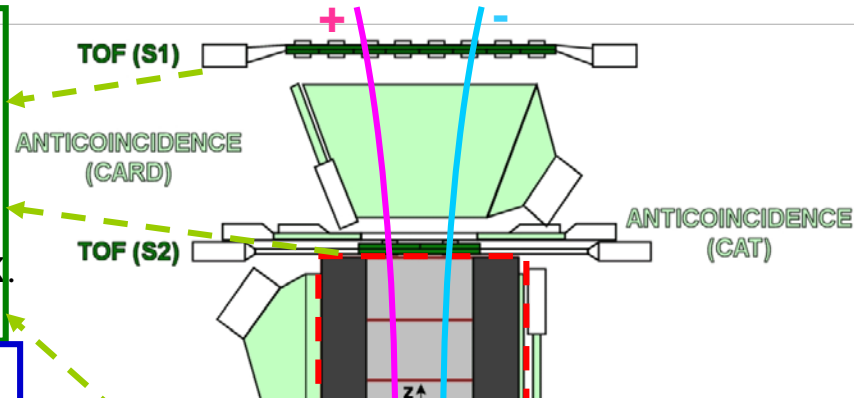


Time-Of-Flight

plastic scintillators + PMT:

- Trigger
- Albedo rejection;
- Mass identification up to 1 GeV;
- Charge identification from dE/dX .

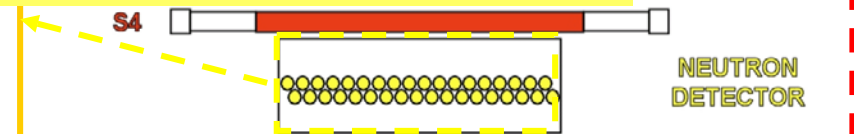
Electromagnetic calorimeter



Launched on 15th June 2006 PAMELA in nearly continuous data-taking mode since then. Recently celebrated 9.5 years!

^3He tubes + polyethylene moderator:

- High-energy e/h discrimination



Spectrometer

microstrip silicon tracking system + permanent magnet

It provides:

- *Magnetic rigidity* → $R = pc/Ze$
- *Charge sign*
- *Charge value from dE/dx*

GF: 21.5 cm² sr

Mass: 470 kg

Size: 130x70x70 cm³

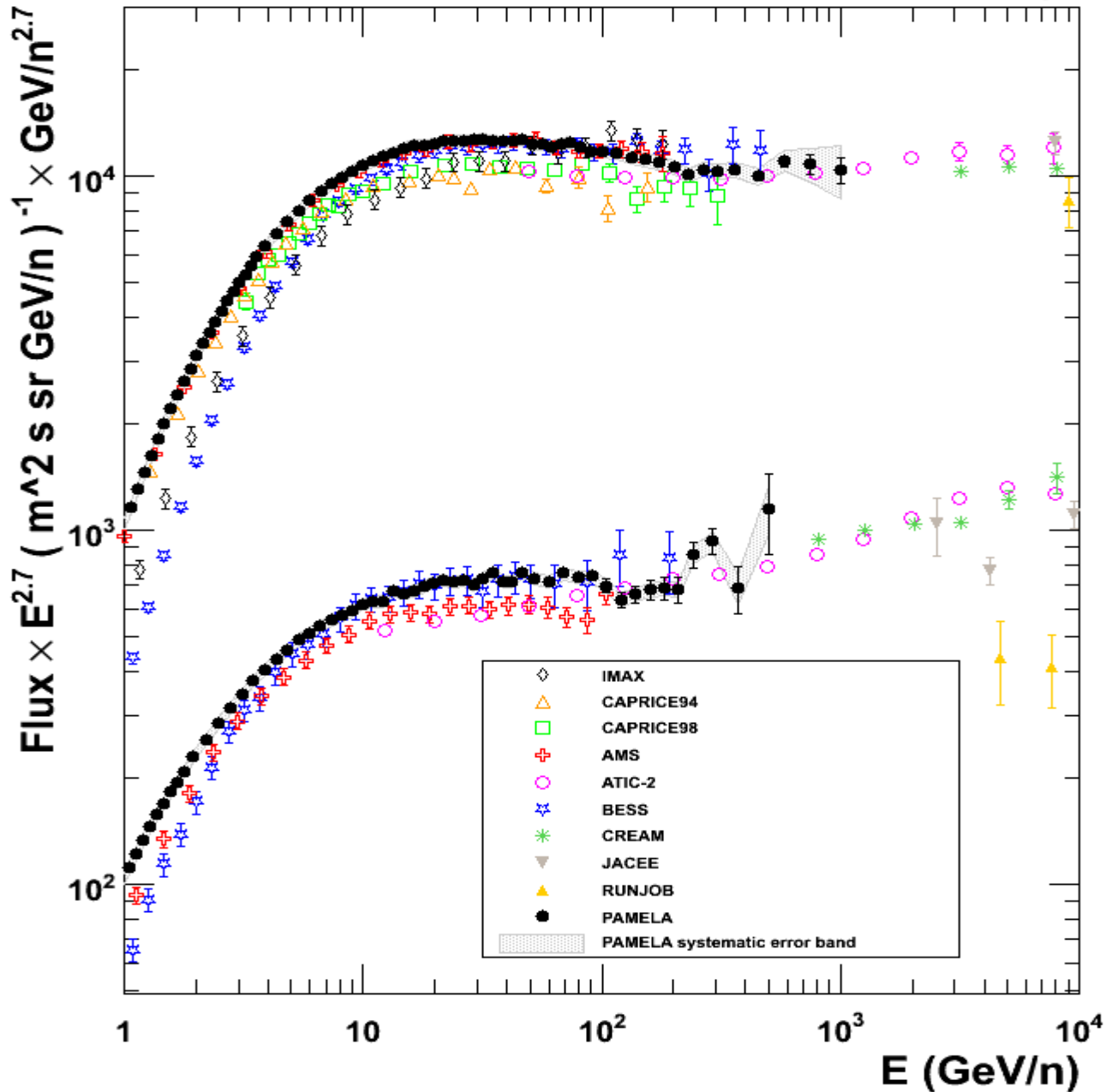
Power Budget: 360W

SPECTROMETER

CALORIMETER

**NEUTRON
DETECTOR**

Proton and Helium Nuclei Spectra



H & He absolute fluxes @ high

energy



Spectral index

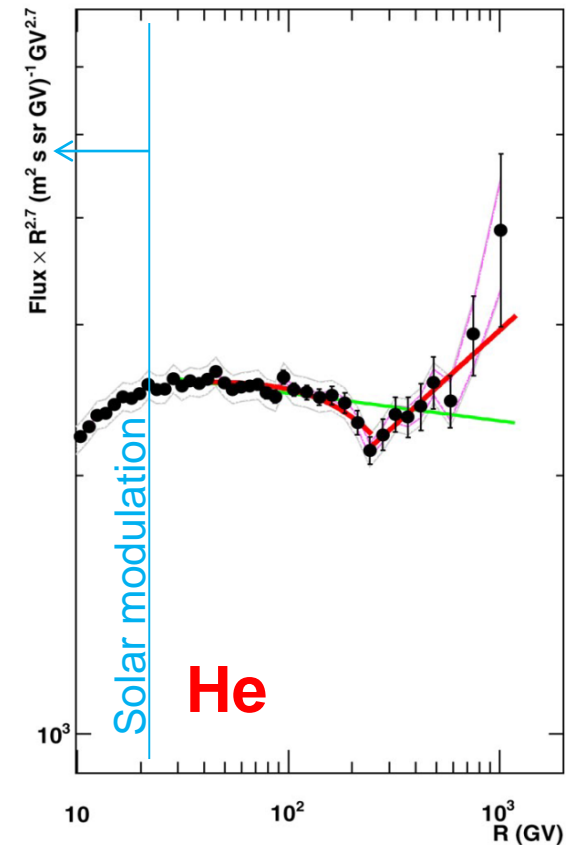
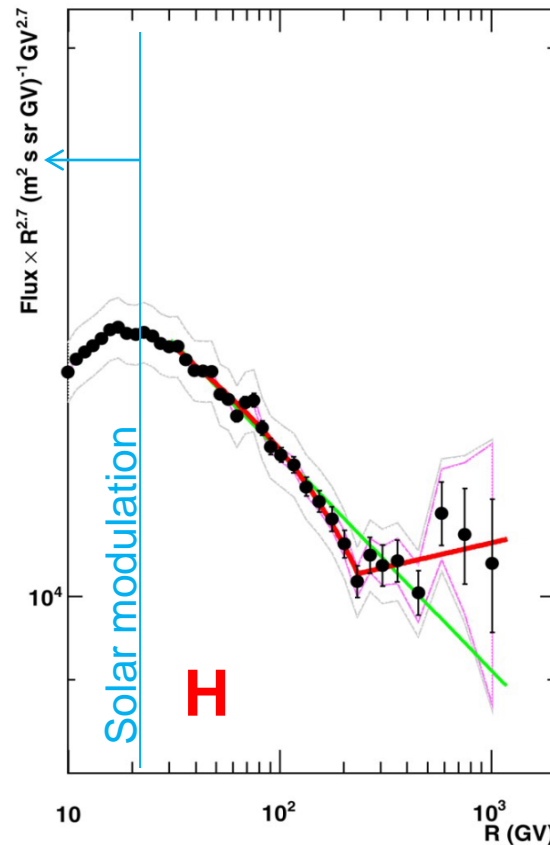


Deviations from single power law (SPL):

- Spectra gradually soften in the range 30÷230GV
 - Spectral hardening @ $R \sim 235\text{GV}$ $\Delta\gamma \sim 0.2 \div 0.3$
- SPL is rejected at 98% CL

Origin of the structures?
(e.g. see P. Blasi, Braz.J.Phys. 44 (2014) 426)

- At the sources: multi-populations, etc.?
- Propagation effects?



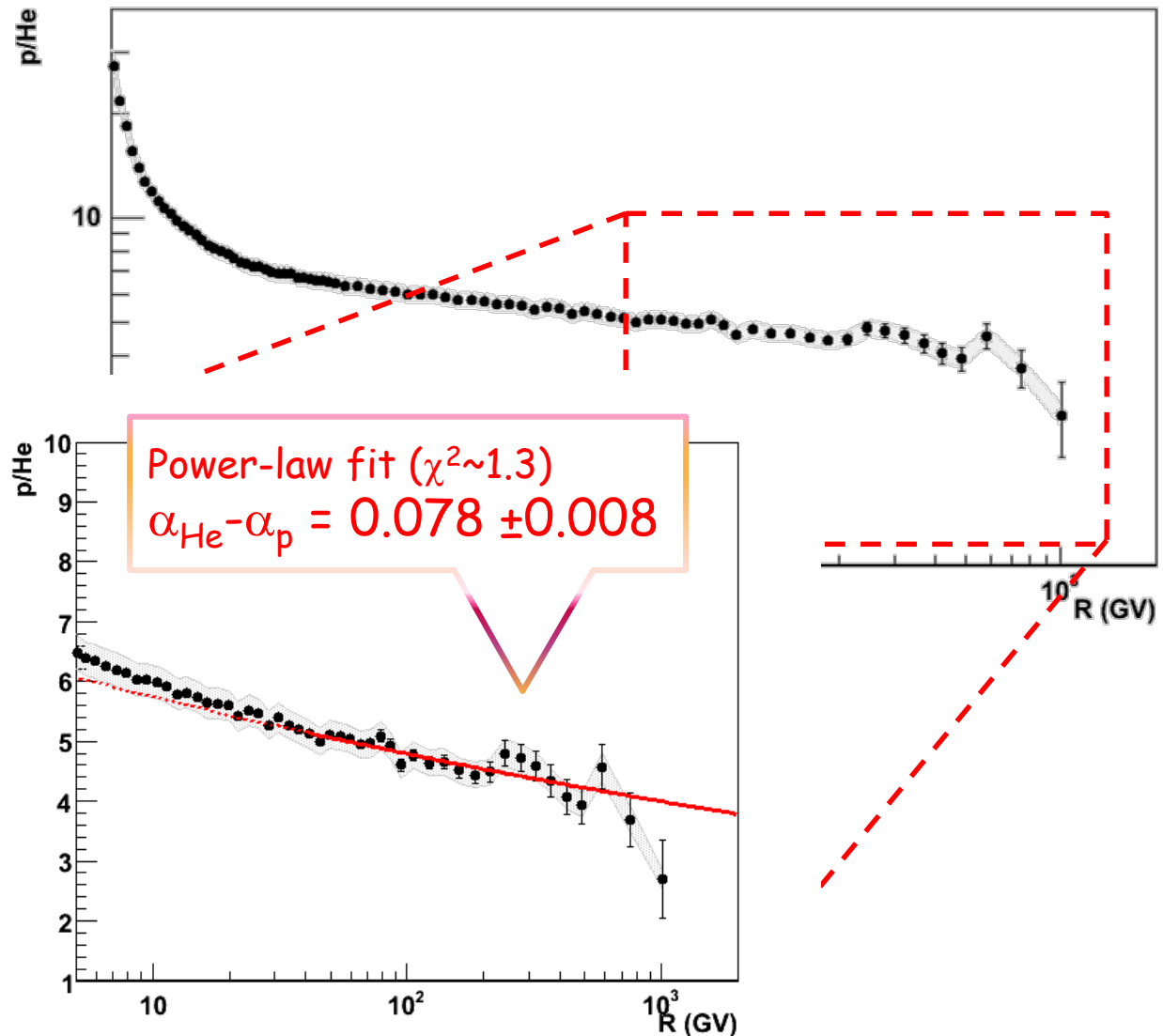
H/He ratio vs R

Instrumental p.o.v.

- Systematic uncertainties partly cancel out

Theoretical p.o.v.

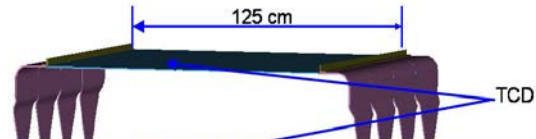
- Spallation effects during propagation:
Blasi & Amato:
arXiv:1105.4521
- acceleration effects:
M. Malkov et al.,
arXiv:1110.5335
- Or?



Detector Systems in CREAM-1

- **TCD: Timing Charge Detector**

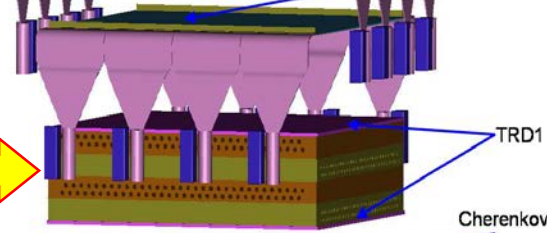
 - ✓ Trigger and Charge



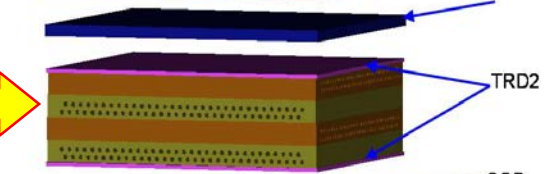
- **TRD: Transition Radiation Detector**

 - ✓ Tracking

 - ✓ Lorentz Factor for $Z \geq 3$



CER: Cherenkov Detector
–Charge/Velocity for $Z \geq 3$



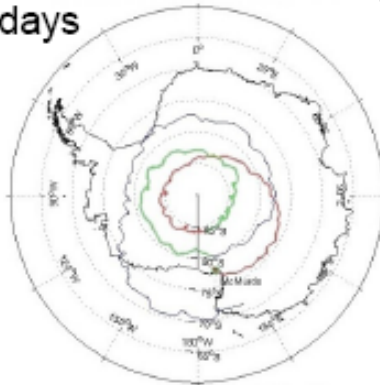
calorimeter module



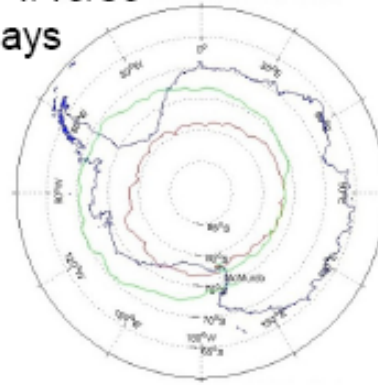
Six Flights: ~ 161 days cumulative exposure



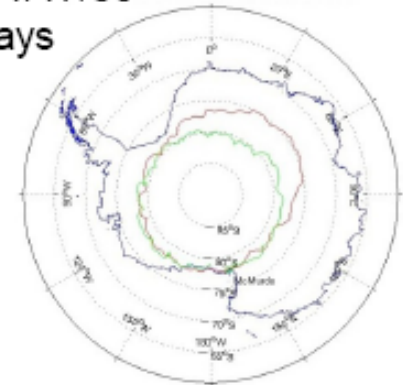
CREAM-I
12/16/04 – 1/27/05
42 days



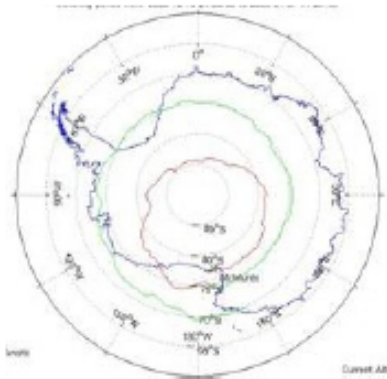
CREAM-II
12/16/05-1/13/06
28 days



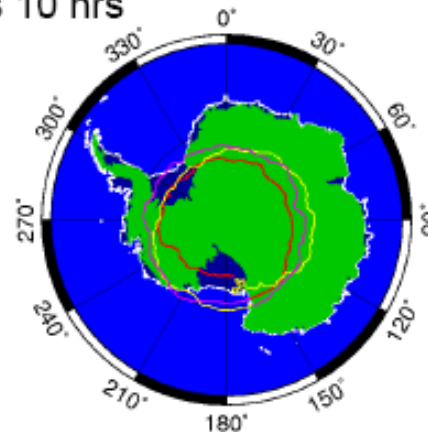
CREAM-III
12/19/07-1/17/08
29 days



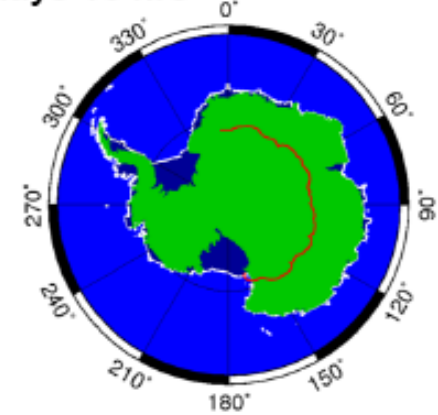
CREAM-IV
12/19/08 - 1/7/09
19 days 13 hrs



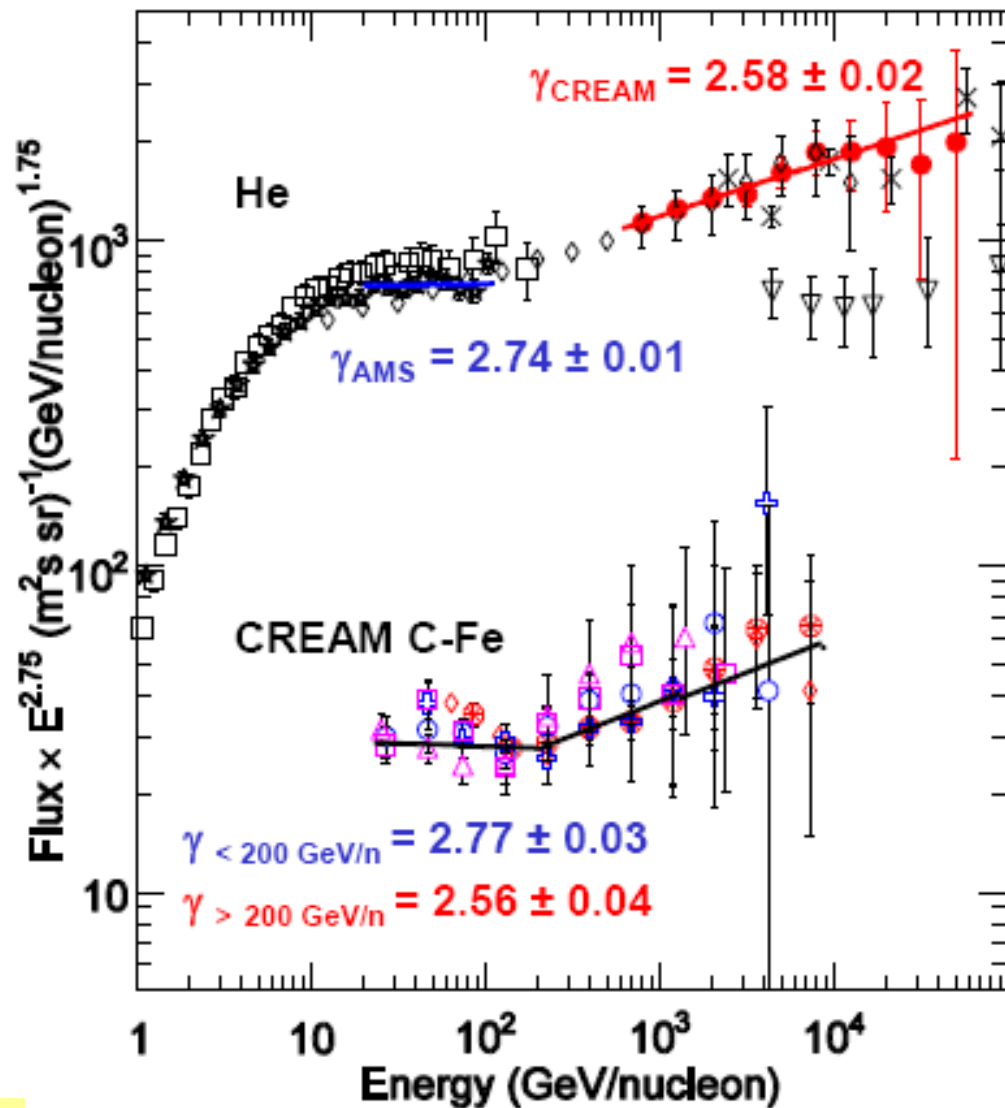
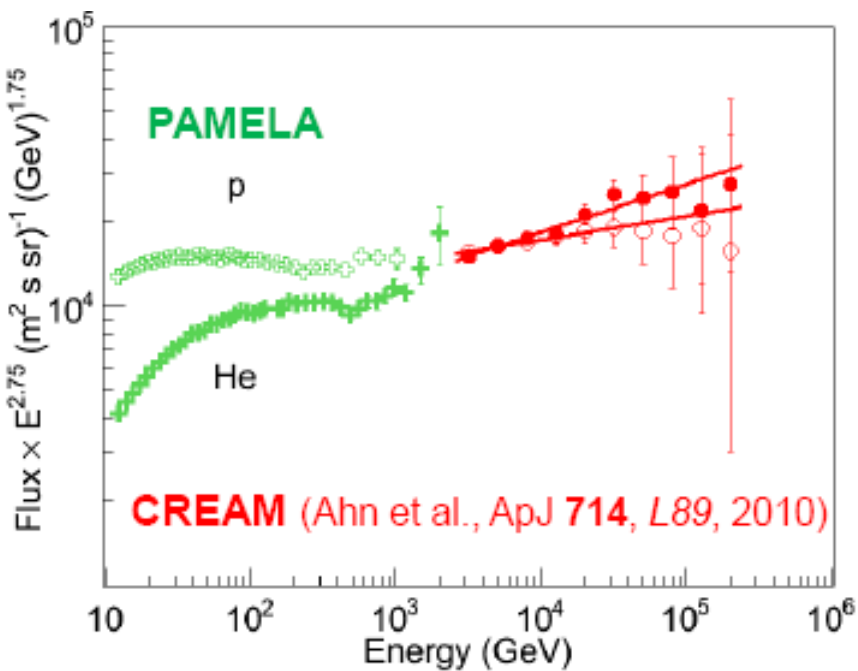
CREAM-V
12/1/09 – 1/8/10
37 days 10 hrs



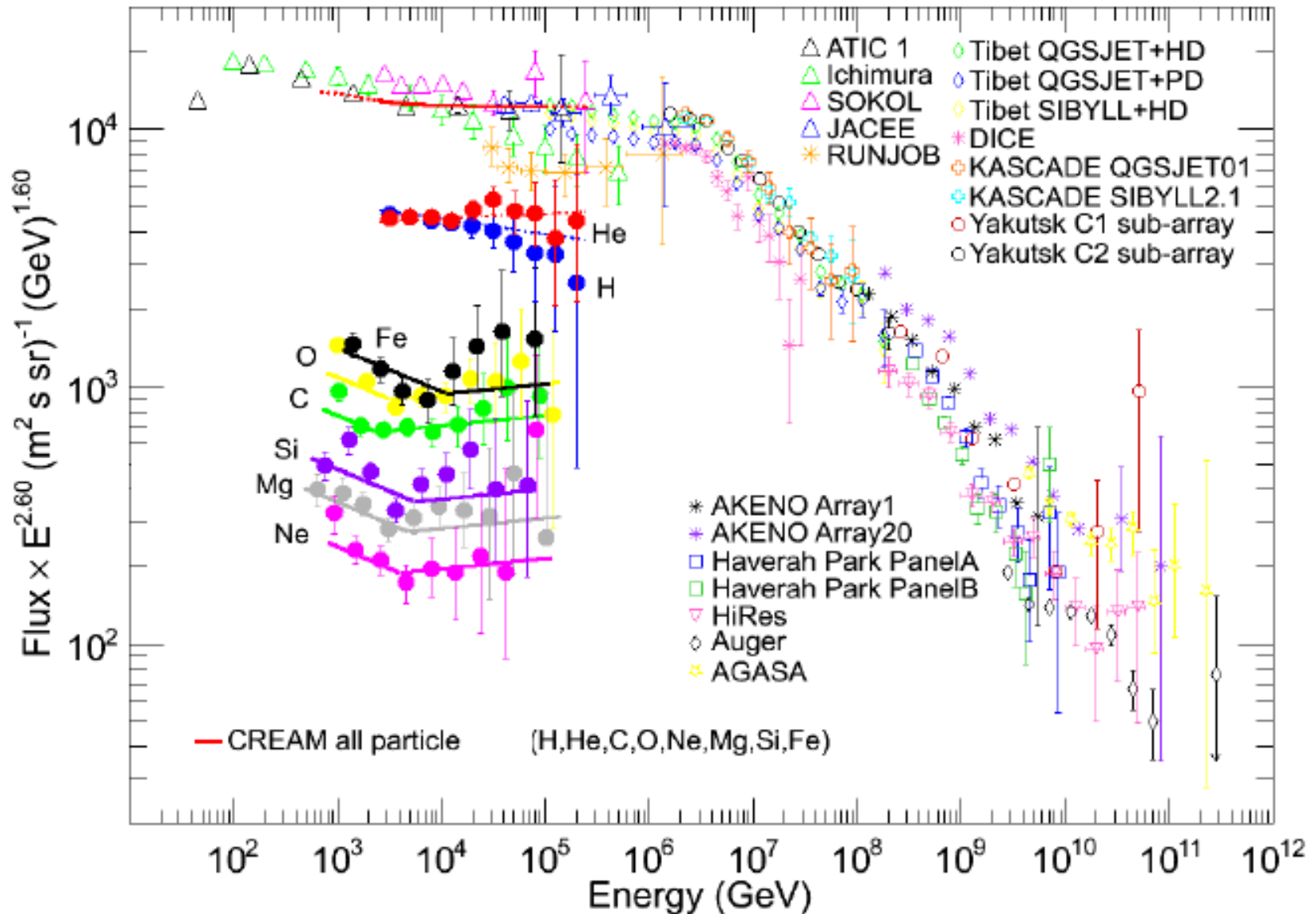
CREAM-VI
12/21/10 – 12/26/10
5 days 16 hrs



CREAM absolute fluxes @ high energy

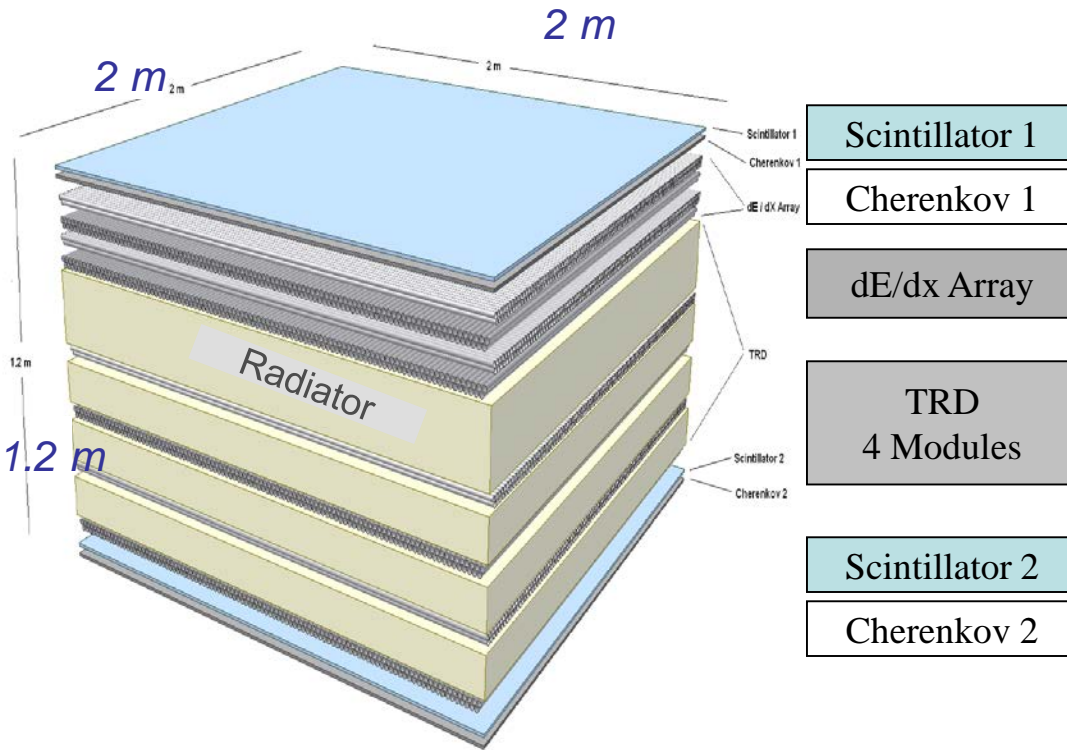


Particle Spectra

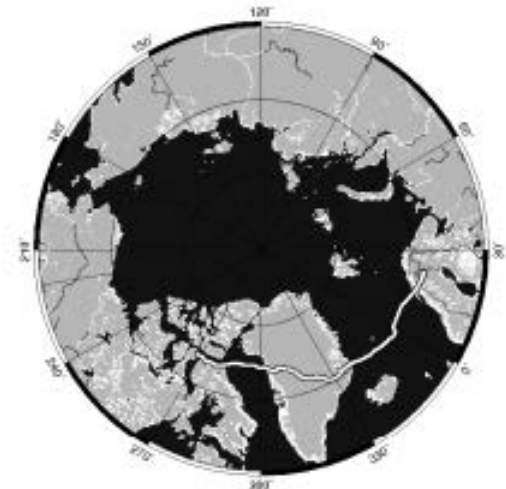
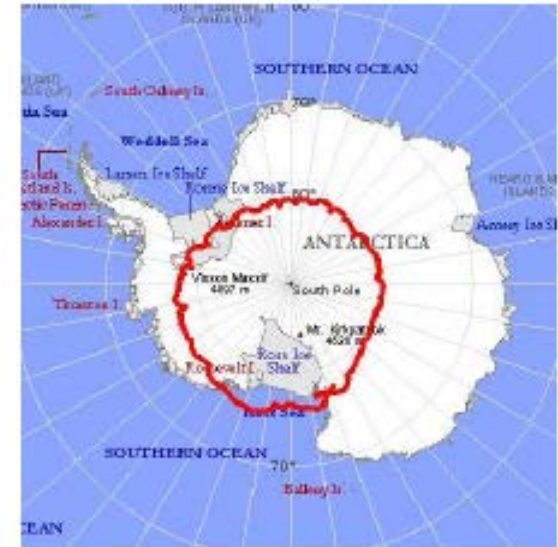


Transition Radiation Array for Cosmic Energetic Radiation

Detector System



*1600 proportional tubes,
2 cm dia, 200 cm long*



Transition radiation

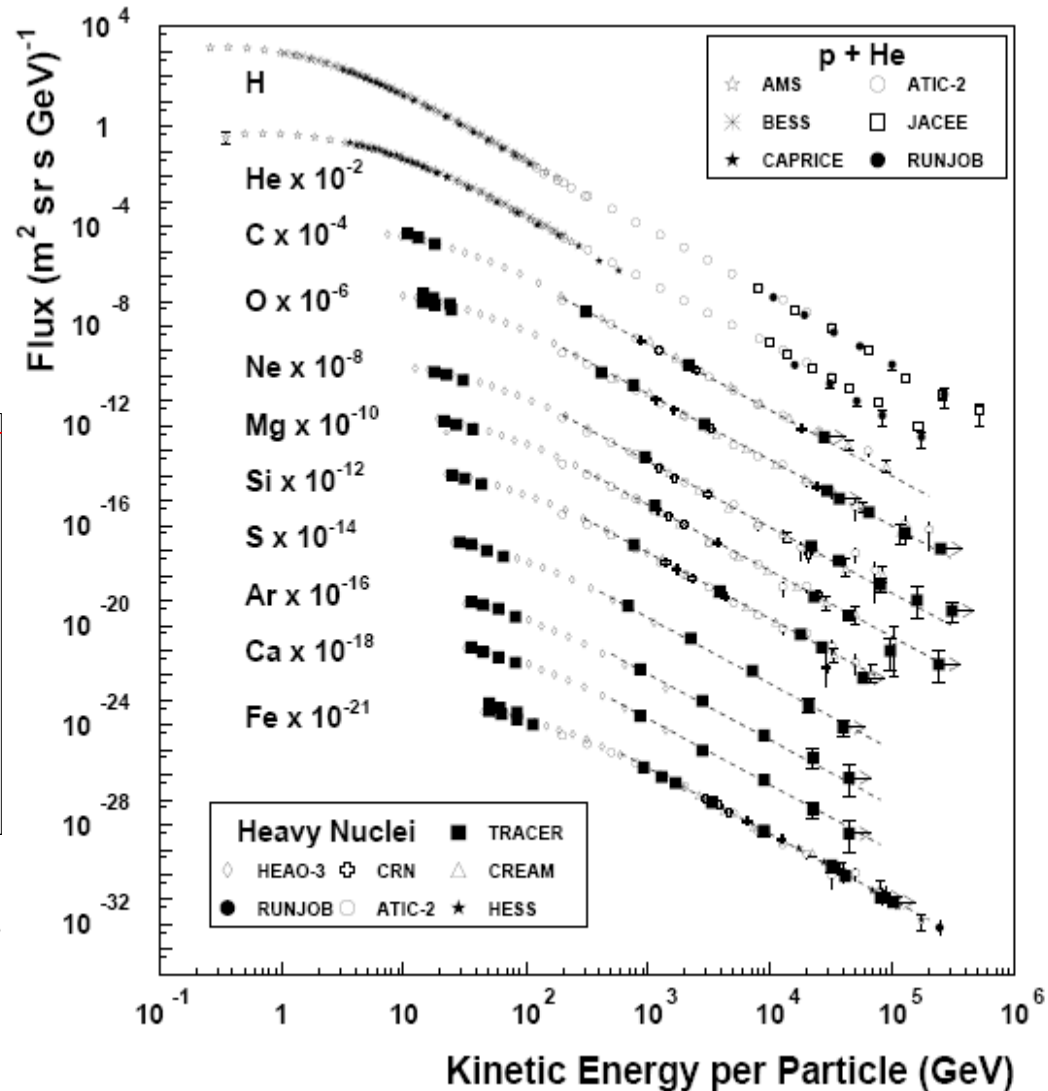
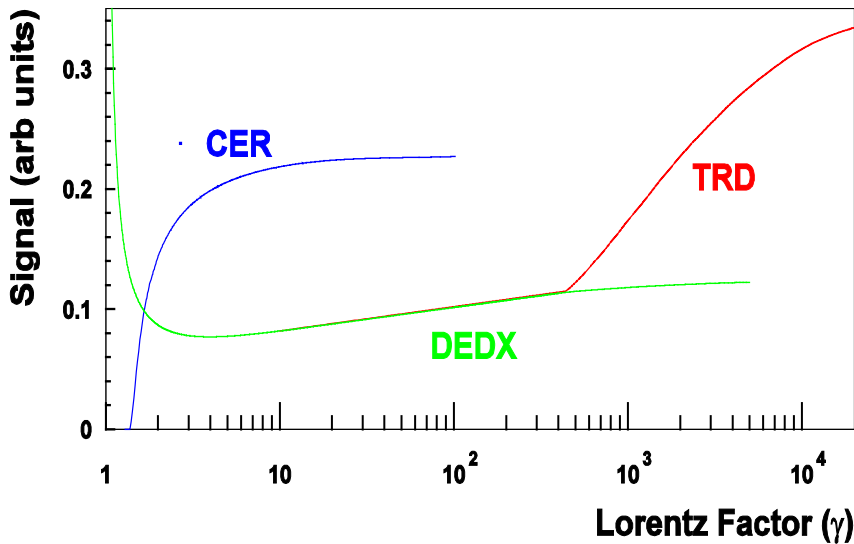
X-ray transition radiation (XTR) occurs when a relativistic charged particle passes from one medium to another of a different dielectric permittivity.

The energy radiated when a particle with charge $z_p e$ and $\gamma \simeq 1000$ crosses the boundary between vacuum and a different transparent medium is typically concentrated in the soft x-ray range 2 keV to 40 keV.

The process is closely related to Cherenkov radiation

TRACER nuclei absolute fluxes (and energy response)

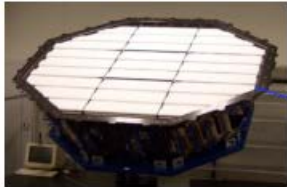
Acrylic Cherenkov Counter ($\gamma < 10$)
Specific Ionization in Gas ($4 < \gamma < 1000$)
Transition Radiation Detector ($\gamma > 400$)



AMS Experiment on ISS

AMS consists of 5 sub-detectors which provide redundant information for particle identification

TRD
Identify e^+ , e^-



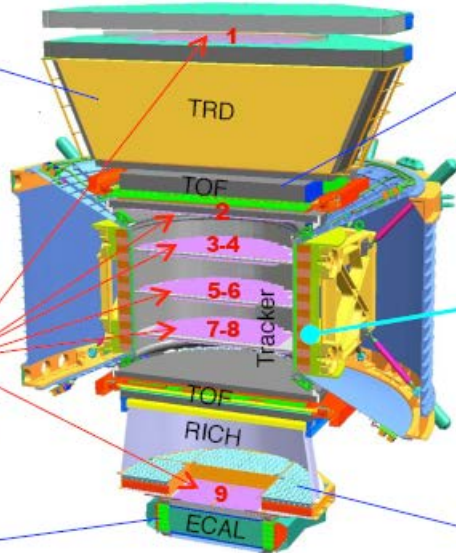
Silicon Tracker
 Z, P



ECAL
 E of e^+ , e^- , γ



Particles and nuclei are defined by their charge (Z) and energy ($E \sim P$)



TOF
 Z, E



Magnet
 $\pm Z$

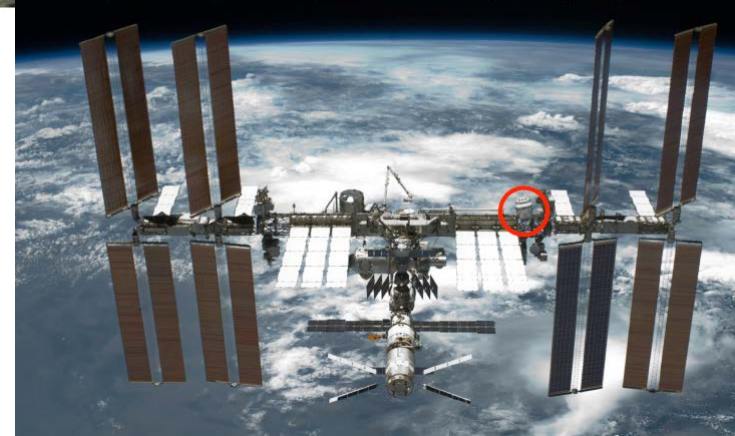


RICH
 Z, E



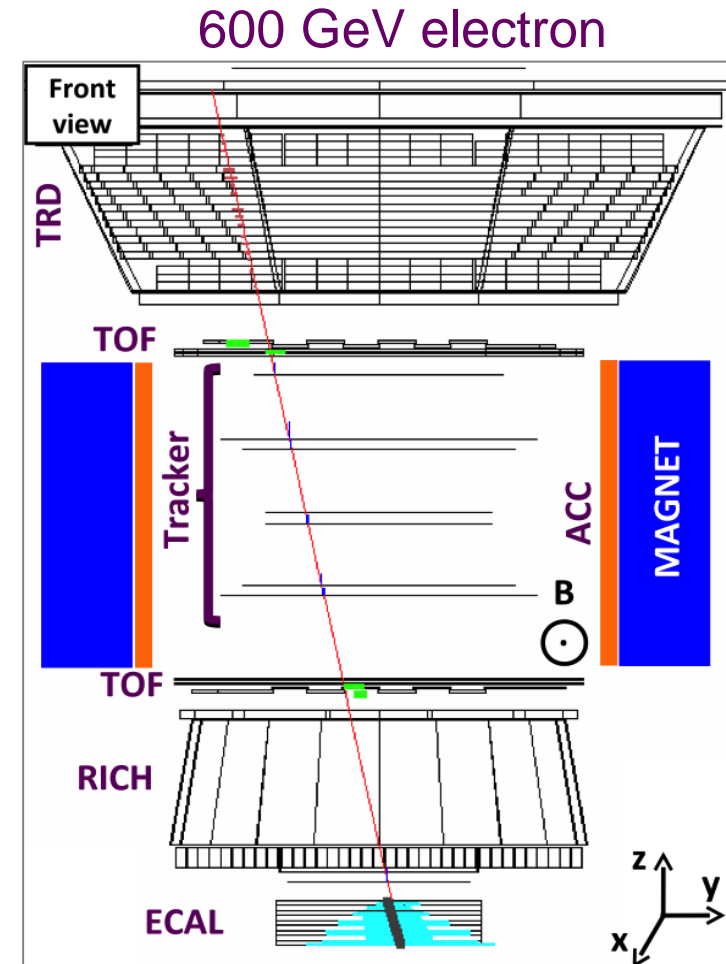
Z, P are measured independently by the Tracker, RICH, TOF and ECAL

The Alpha Magnetic Spectrometer (AMS) Experiment



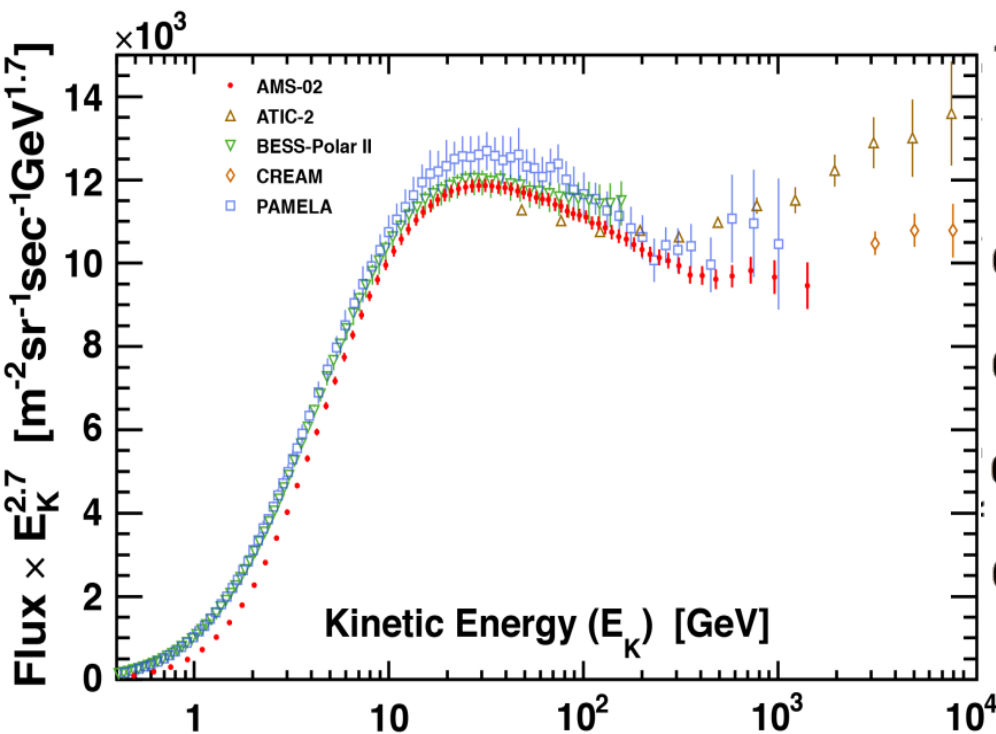
Full coverage of anti-matter & CR physics

	e^-	P	He, Li, Be,...Fe	γ	e^+	\bar{P}	\bar{He}, \bar{C}
TRD							
TOF							
Tracker +Magnet							
RICH							
ECAL							
Physics example	Cosmic Ray Physics				Dark matter		Anti matter

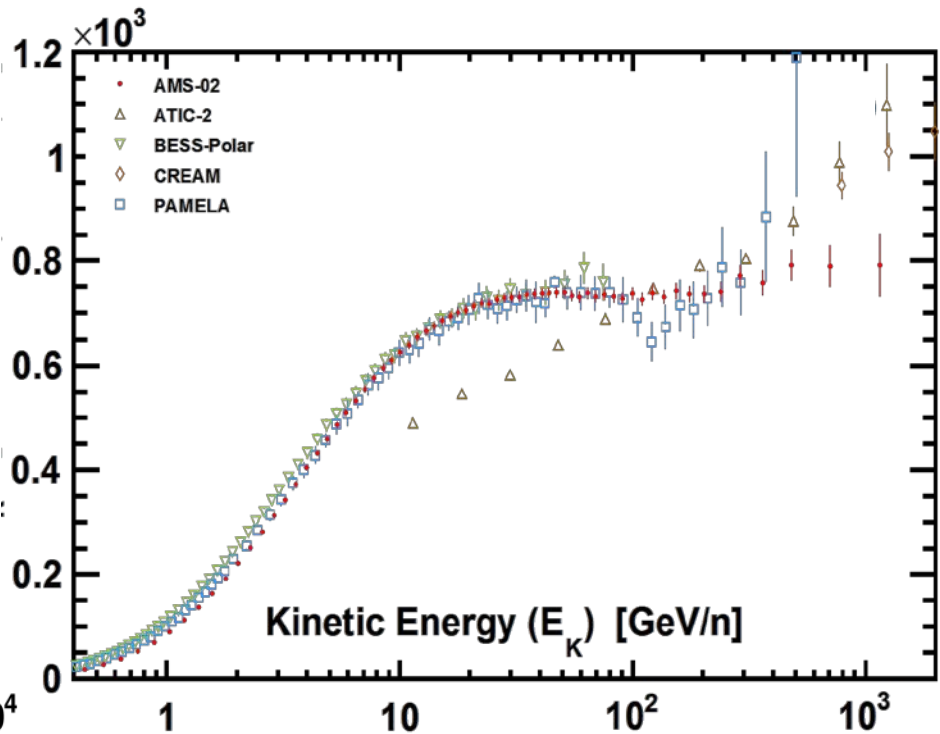


AMS H and He fluxes

AMS-02 H flux measurement:
300 million events



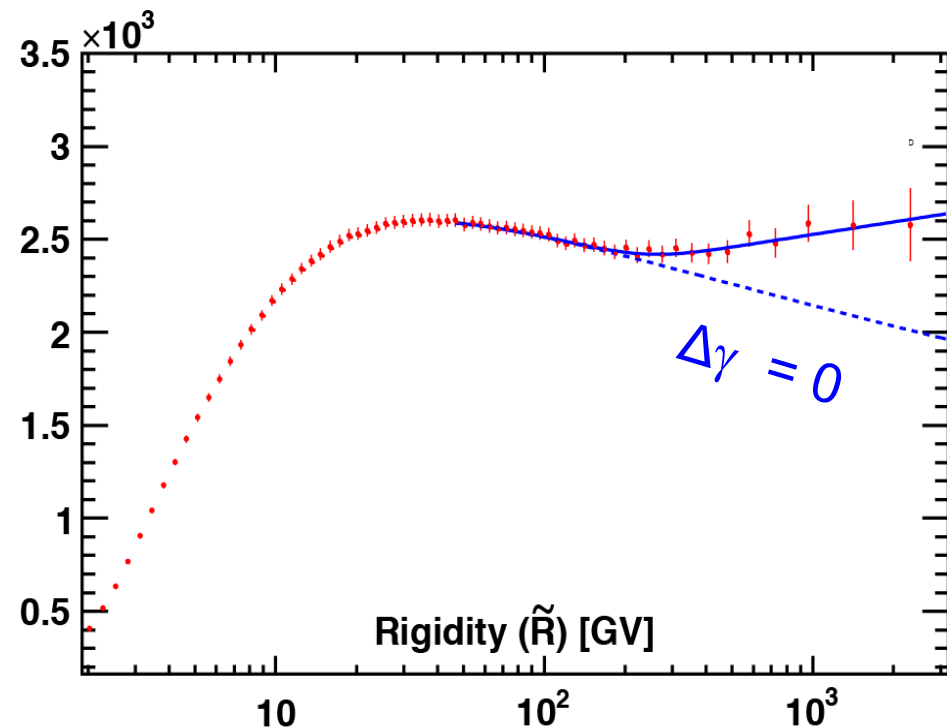
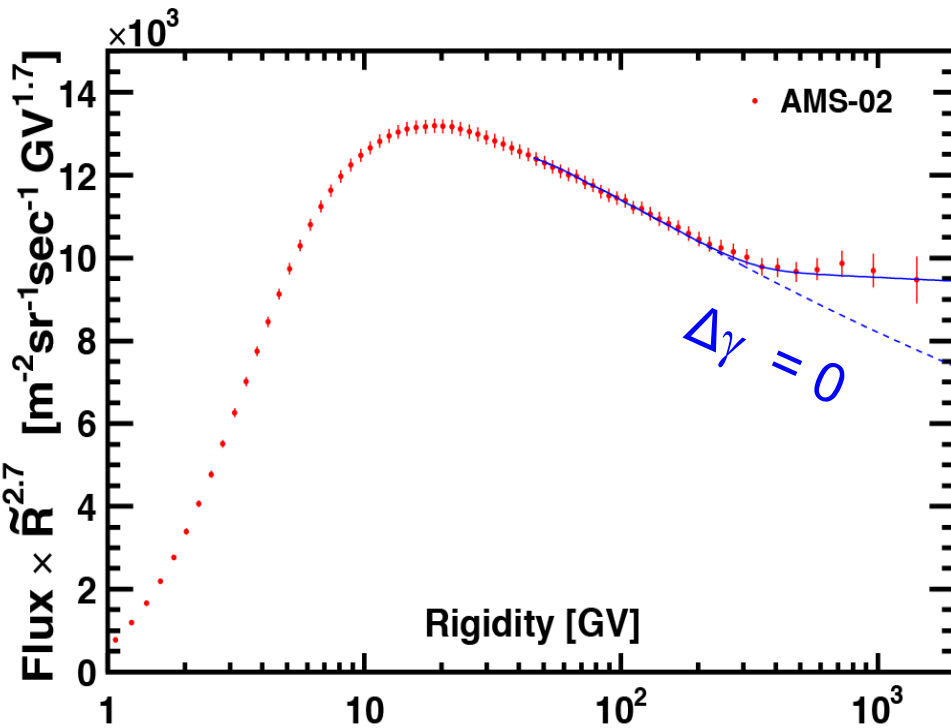
AMS-02 He flux measurement:
50 million events



AMS H and He fluxes

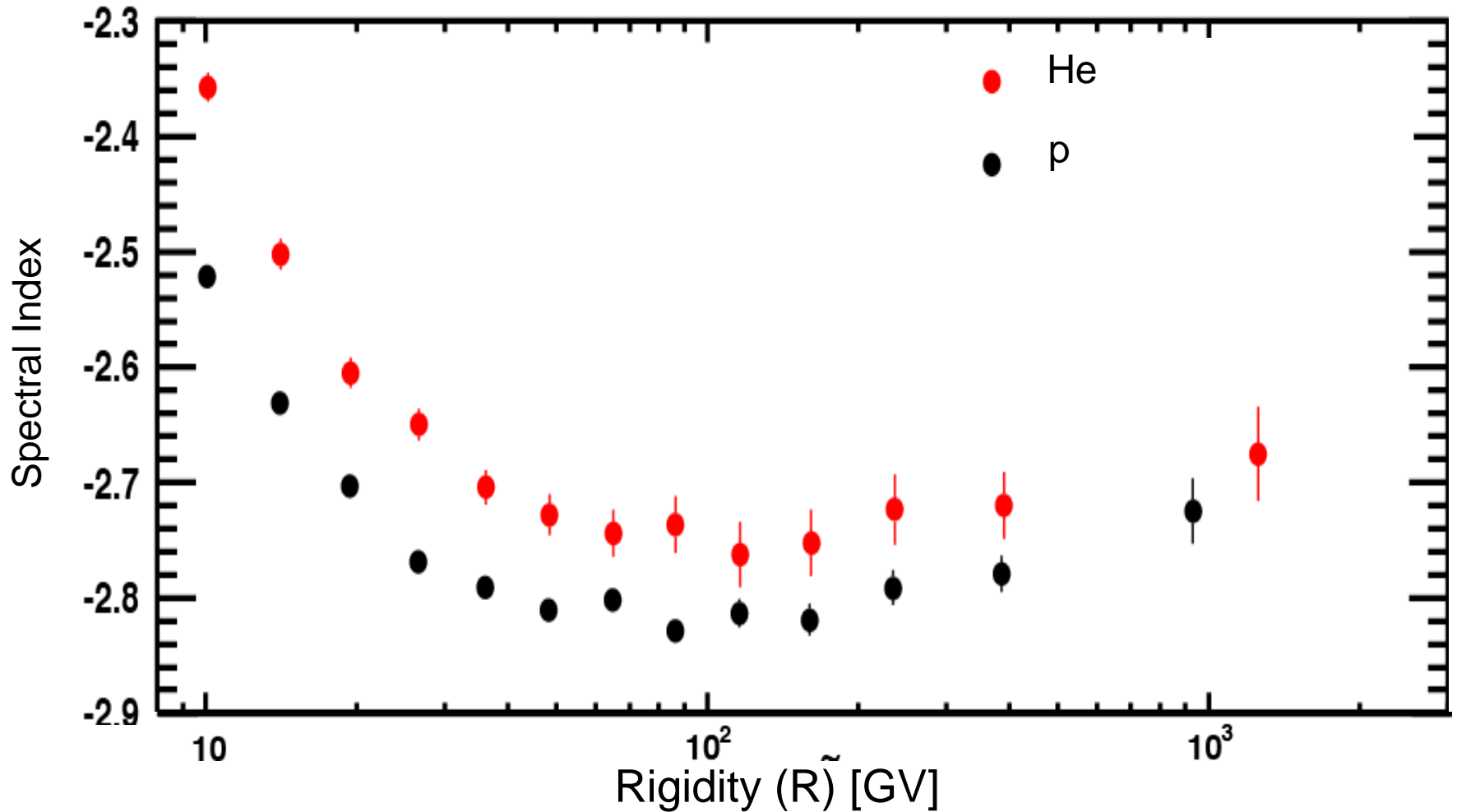
Two power laws $R^\gamma, R^{\gamma+1}$ with a characteristic transition rigidity R_0 and a smoothness parameter s well describe H, He measured spectra:

$$\Phi = C \left(\frac{R}{45GV} \right)^\gamma \left[1 + \left(\frac{R}{R_0} \right)^{\Delta\gamma/s} \right]^s$$

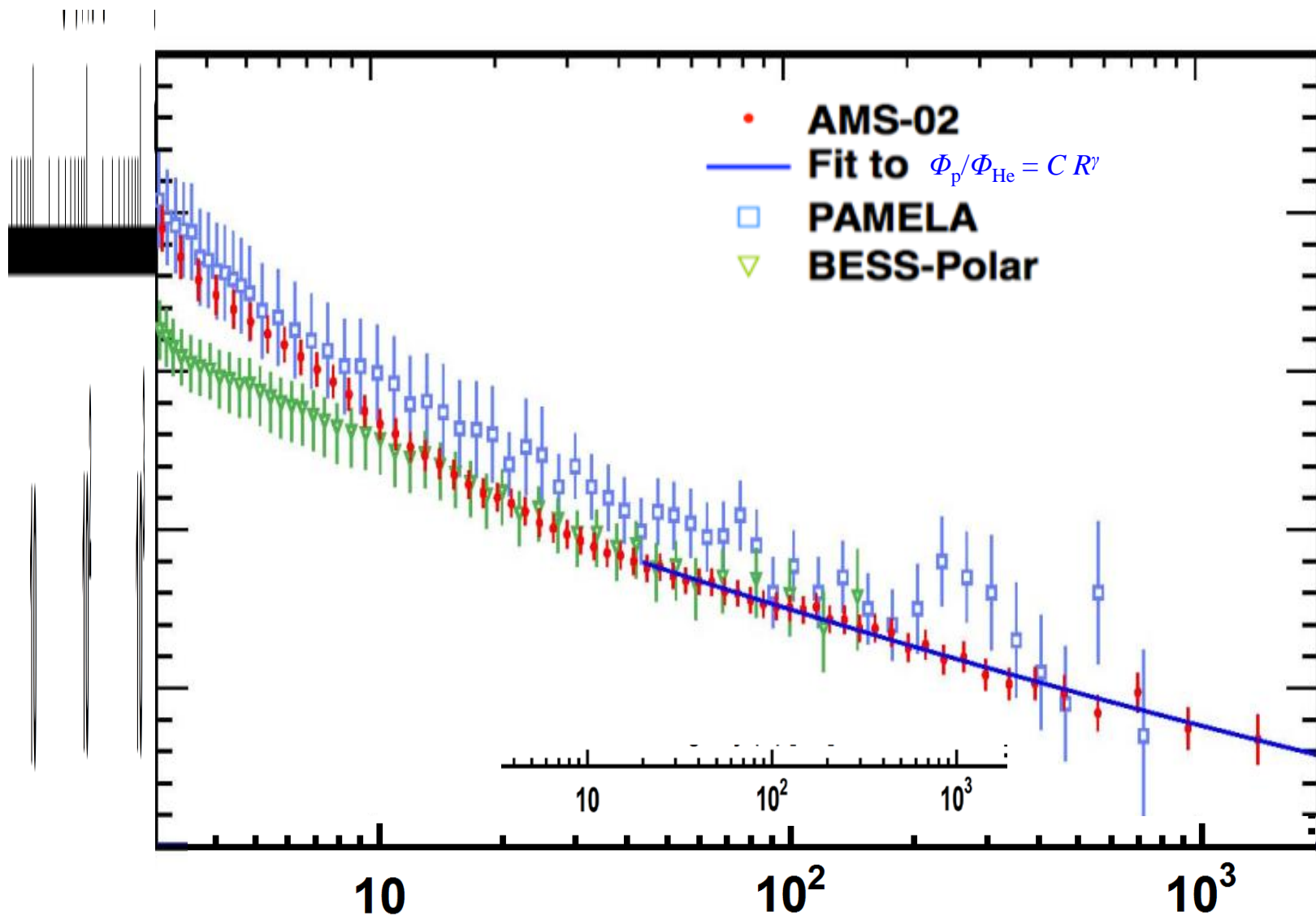


Model Independent Spectral Indices Comparison

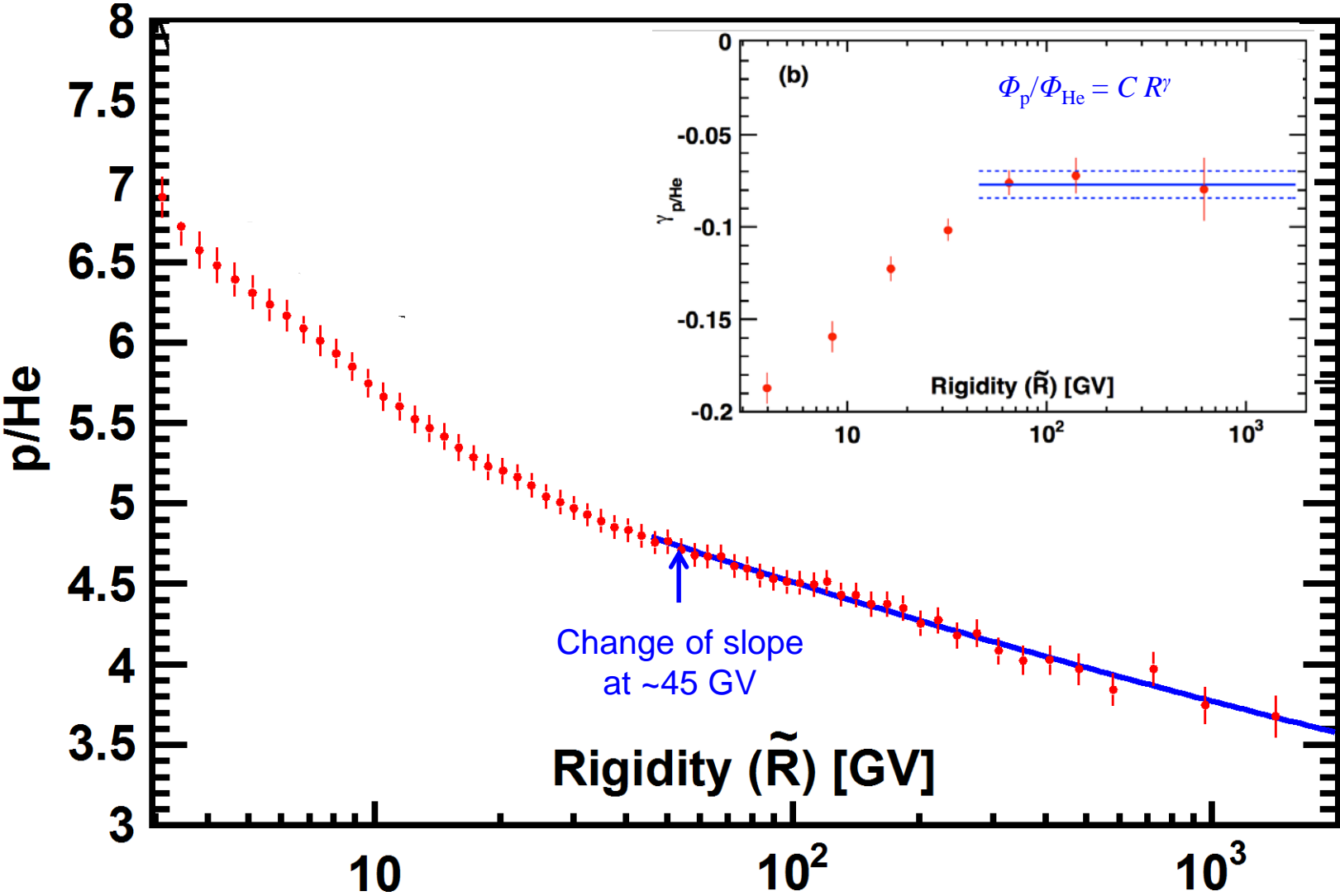
$$\gamma = d \log (\Phi) / d \log (R)$$



AMS p/He flux ratio

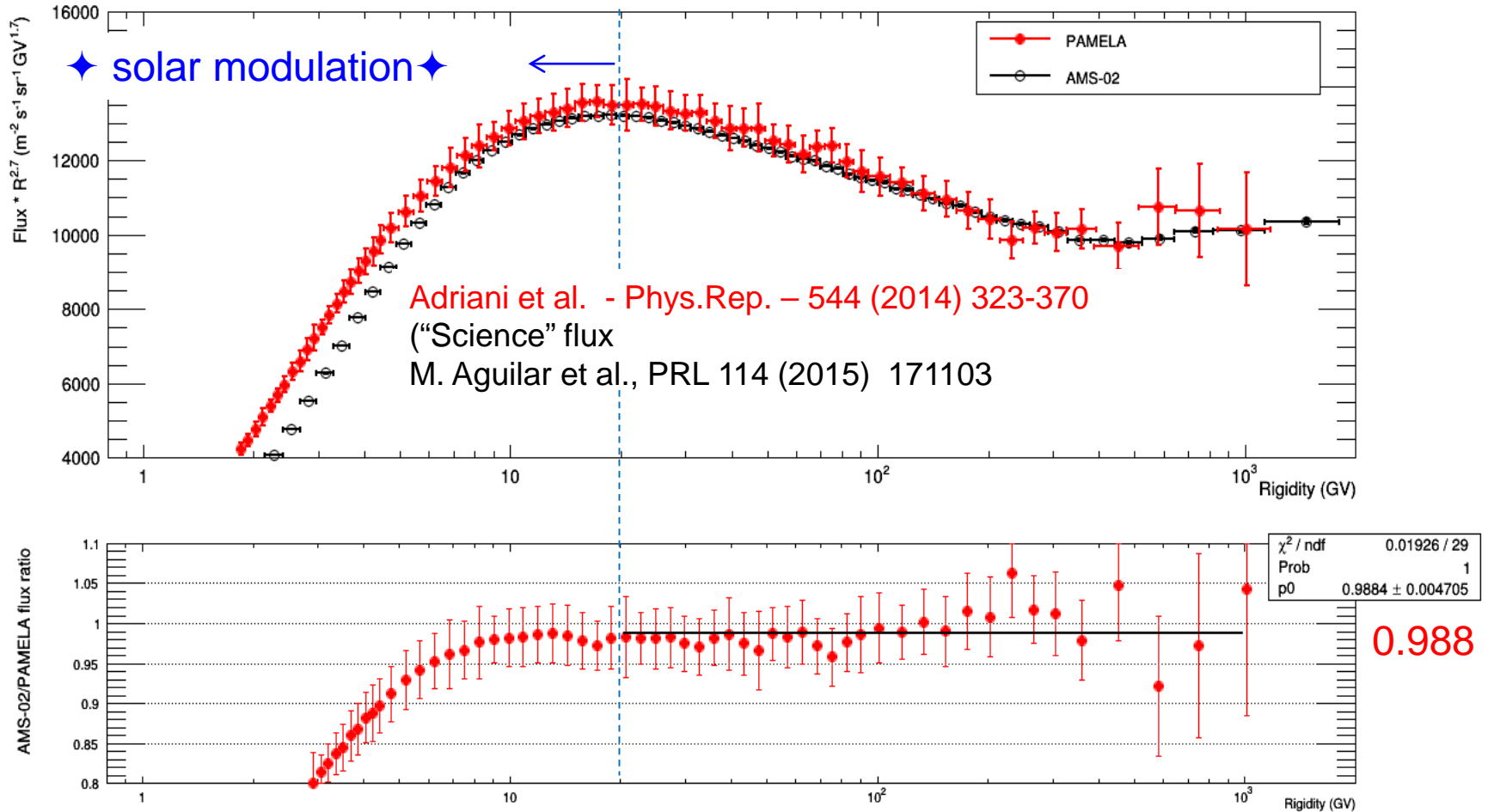


AMS p/He flux ratio



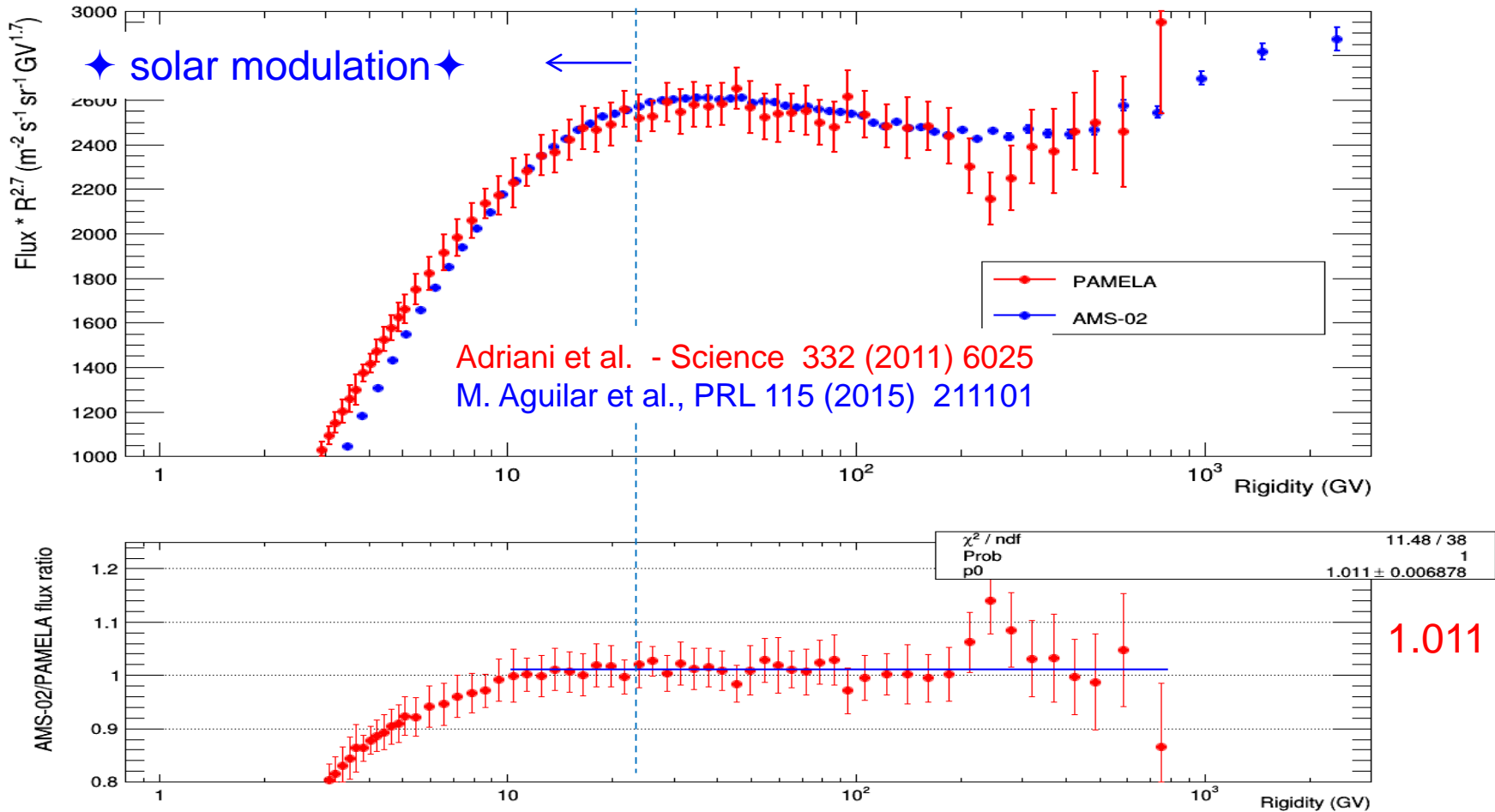
PAMELA vs AMS02

PAMELA data → Jul 2006 ÷ Mar 2008
AMS02 data → May 2011 ÷ Nov 2013

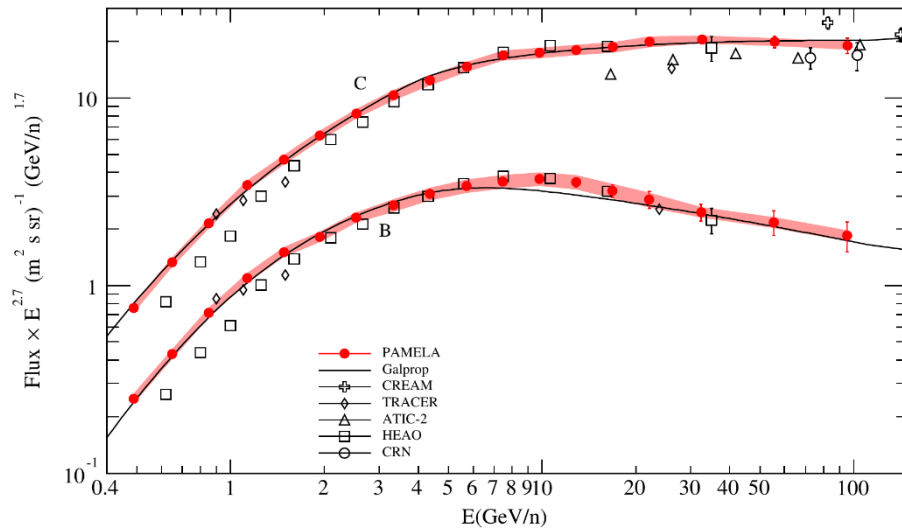


PAMELA vs AMS02

PAMELA data → Jul 2006 ÷ Mar 2008
AMS02 data → May 2011 ÷ Nov 2013



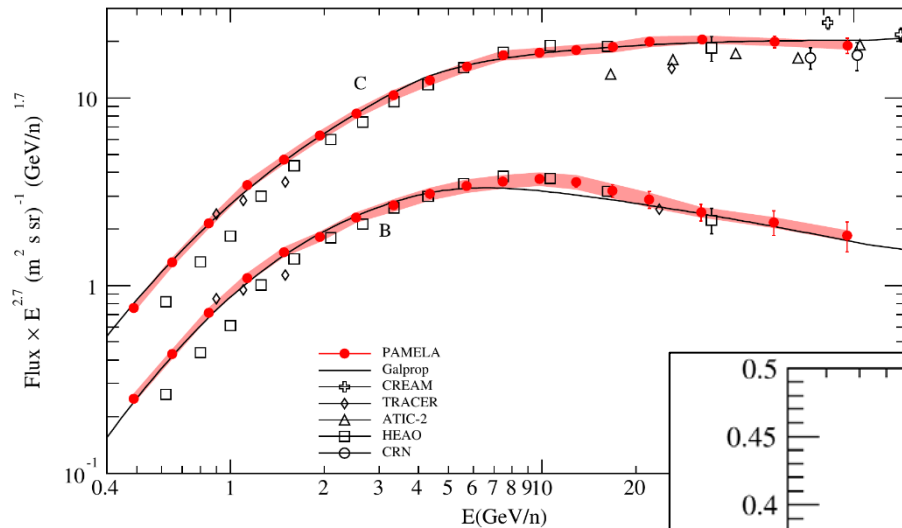
Boron and carbon fluxes and B/C



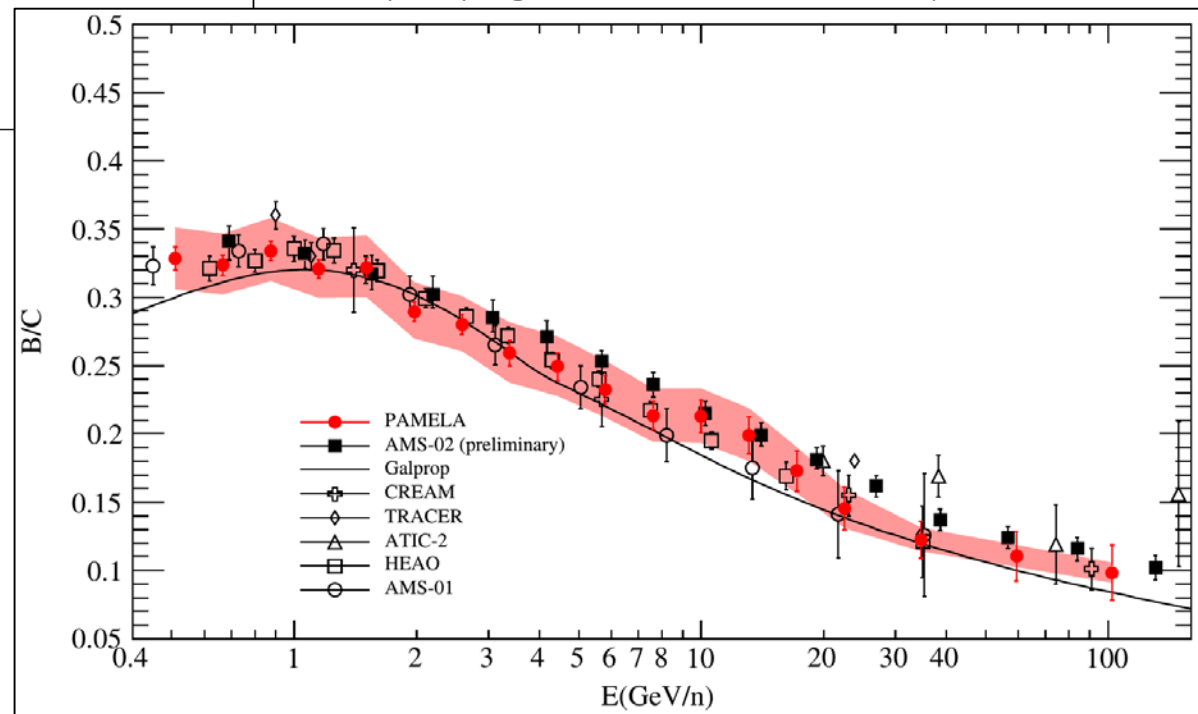
- Tracking performance:
 - $\sigma_x = 14 \mu\text{m}$, $\sigma_y = 19 \mu\text{m}$
 - $\text{MDR} = 250 \text{ GV}$
- Modelization of cosmic-ray propagation in the *Galaxy*

Adriani et al., ApJ 791 (2014), 93

Boron and carbon fluxes and B/C



- Tracking performance:
 - $\sigma_x = 14 \mu\text{m}$, $\sigma_y = 19 \mu\text{m}$
 - MDR = 250 GV
- Modelization of cosmic-ray propagation in the Galaxy



Adriani et al., ApJ 791 (2014), 93

AMS-02 and others: B/C and Boron and carbon fluxes

